Rietveld Profile Functions

James A. Kaduk
Illinois Institute of Technology
North Central College
Kaduk@polycrystallography.com

Mottoes for the powder diffractionist

- It depends
- Overlap kills
- *Everything*'s a sample
- Desperate analysts do desperate things
- If you have a single crystal, you should use it

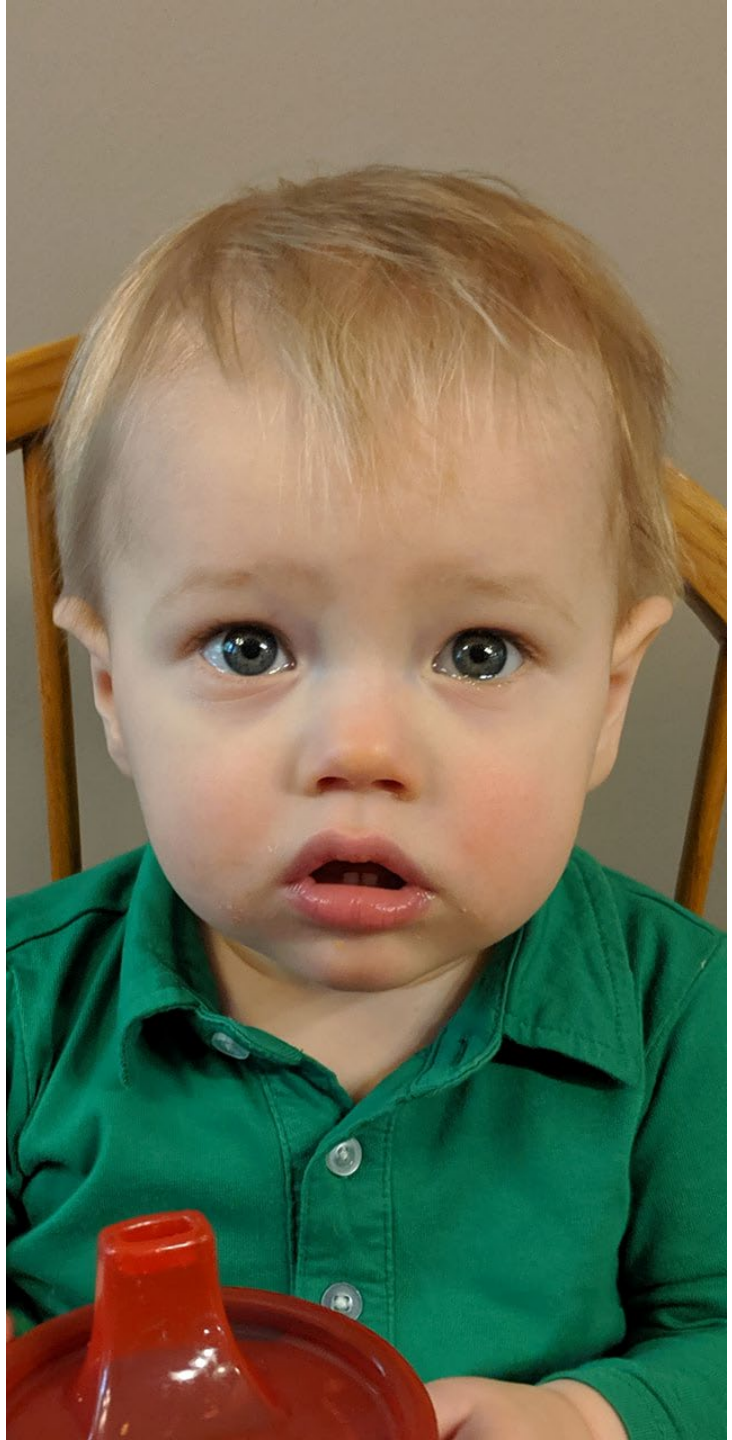


TOWN

Convolution

$$(f * g)(t) = \int_{-\infty}^{\infty} f(\tau) \cdot g(t-\tau) d\tau = \int_{-\infty}^{\infty} f(t-\tau) \cdot g(\tau) d\tau$$

The Fundamental Parameters approach

http://en.wikipedia.org/wiki/Convolution

Convolution

- Convolution of one function (input) with a second function (impulse response) gives the output of a system
- A weighted moving average
- In optics, “blur” is described by convolution

BHT working on convolution to generate instrument parameters

ESRF BM16 (now ID22) Second Monochromator Crystal Rocking Curve

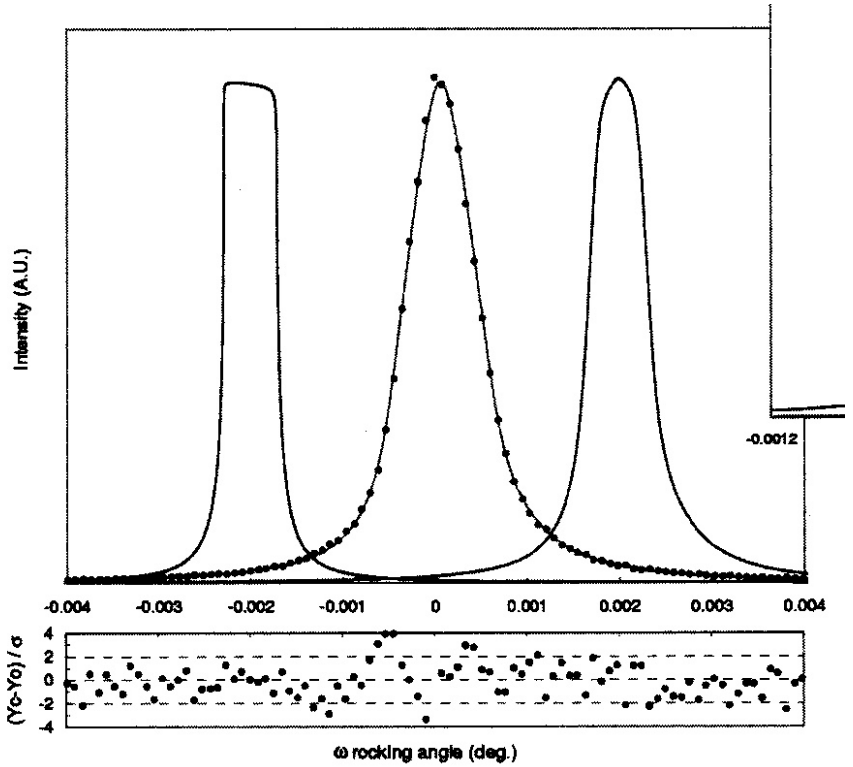

Left; perfect Si(111) Darwin profile. Right: perfect Si(111) reflection convoluted with first crystal strain function. Center: experimental data and fit by convolution of left and right curves.

O. Masson, E. Dooryhee, and A. N. Fitch, “Instrument line-profile synthesis in high-resolution synchrotron powder diffraction”, J. Appl. Cryst., 36, 286-294 (2003).

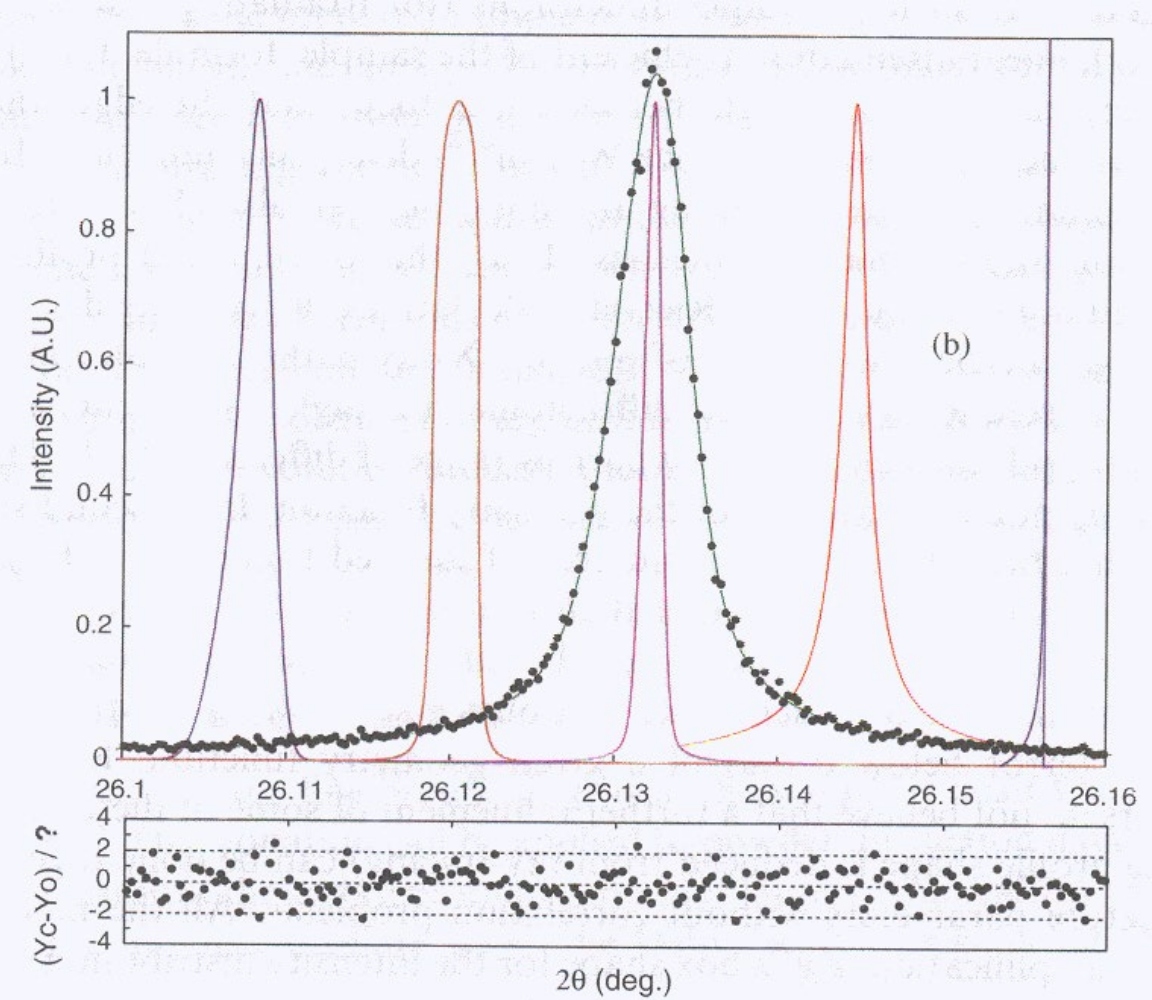

$Na_2Ca_3Al_2F_{14}$ (921) reflection. From left to right: the incident beam source profile, the transfer function of the monochromator, the pure sample profile, the reflection profile of the analyzer, and the axial divergence asymmetry function.

Masson, Dooryhee, and Fitch, in A. Le Bail, "The Profile of a Bragg Reflection for Extracting Intensities", in R. E. Dinnebier and S. J. L. Billinge, *Powder Diffraction: Theory and Practice*, RSC Publishing (2008).

Bragg-Brentano Diffractometer

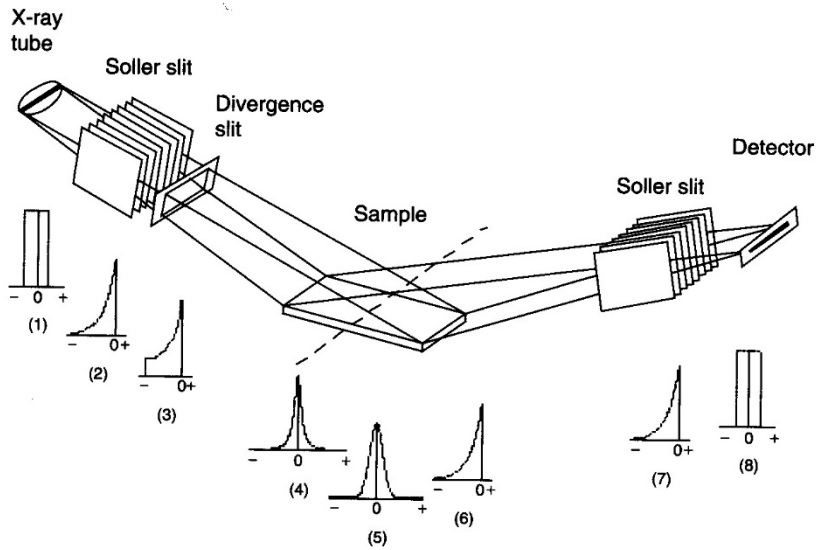

Figure 4.25 Schematic representation of the fundamental parameters approach for a divergent beam diffractometer showing the principal optical components and the sample together with their related aberration functions as discussed in Section 2.2.2 including (1) finite X-ray source width, (2) primary axial divergence, (3) horizontal divergence, (4) crystallite size, (5) strain, (6) absorption, (7) secondary axial divergence and, (8) receiving slit width. Figure copyright Bruker AXS.

A. Kern, "Profile Analysis", in A. Clearfield, J. Reibenspies, and N. Bhuvanesh, *Principles and Applications of Powder Diffraction*, Wiley (2008).

Profile Contributions

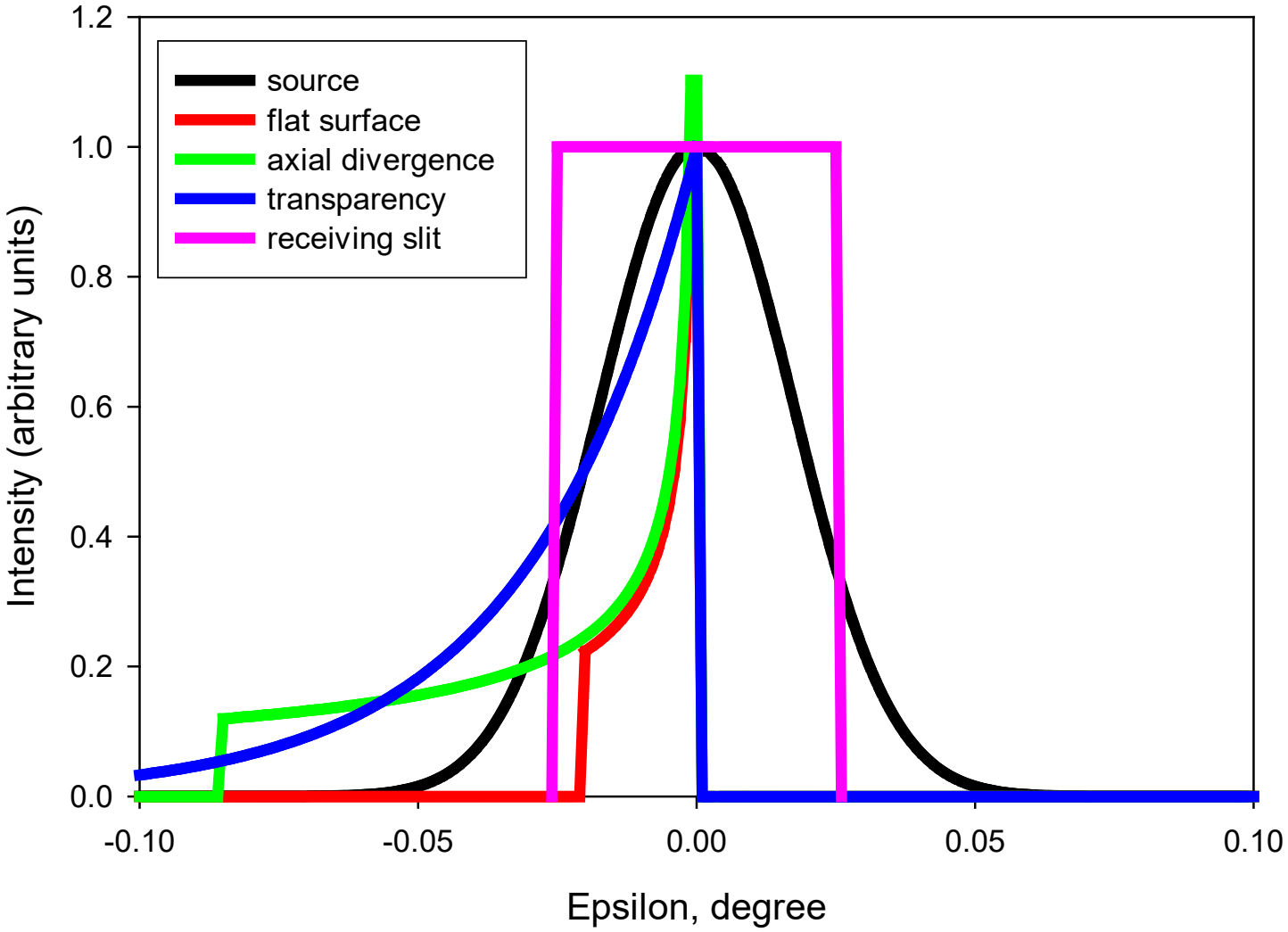

Profile Contributions

Effect	Equation	Range
X-ray Source	$\exp(-k_1^2\varepsilon^2)$ $k_1 = 1.67(\text{FWHM})$	$-\infty$ to $+\infty$
Flat Surface	$\lvert\varepsilon\rvert^{-1/2}$	$-(\gamma^2\cot\theta)/114.6$ to 0 γ = divergence
Axial Divergence	$\lvert 2\varepsilon\cot\theta\rvert^{-1/2}$	$-(\delta^2\cot\theta)/(4\times57.3)$ to 0 δ = axial divergence
Transparency	$\exp(k_4\varepsilon)$ $k_4 = (4\mu R/114.6)\sin2\theta$	$-\infty$ to 0
Receiving Slit		-(FWHM)/2 to + (FWHM)/2

H. P. Klug and L. E. Alexander, *X-ray Diffraction Procedures,* Wiley (1974).

Plus the Cu K_{α} Profile

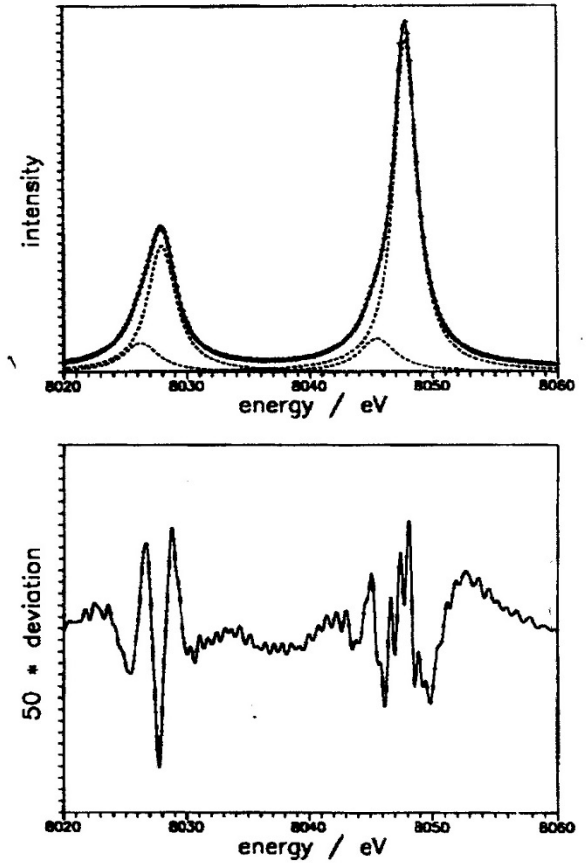

Fig. 4. Top: Cu *Kα* spectrum measured at the Si 444 reflection with the single-crystal spectrometer (crosses) and fitted curve (solid) consisting of four Lorentzians (dotted); bottom: absolute deviation of the fitted curve (50 times enlarged)

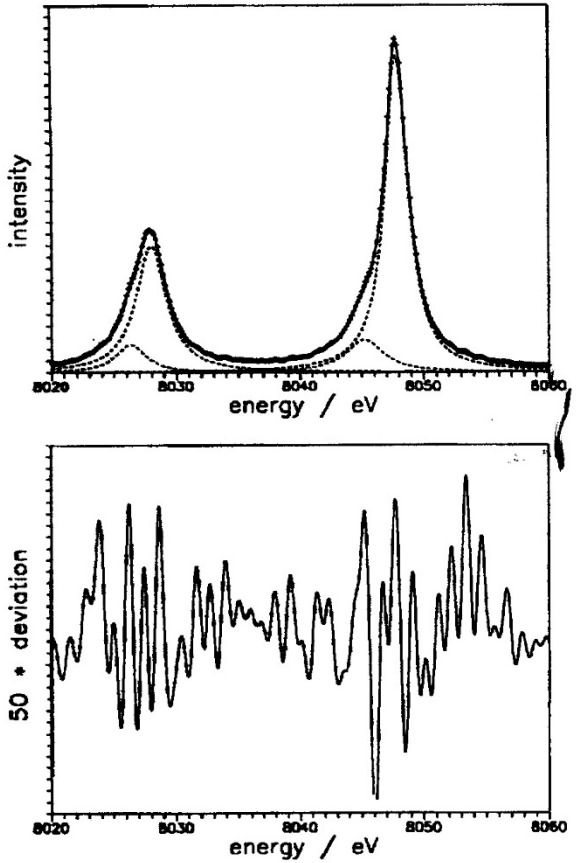

Fig. 5. Top: Cu *Kα* spectrum measured at the Si 333 reflection with the double-crystal spectrometer (crosses) and fitted curve (solid) consisting of four Lorentzians (dotted); bottom: absolute deviation of the fitted curve (50 times enlarged)

J. Hartwig, G. Hölzer, J. Wolf, and E. Förster, "Remeasurement of the Profile of the Characteristic Cu Kα Emission Line with High Precision and Accuracy", *J. Appl. Cryst.,* **26**, 539-548 (1993).

More on Emission Profiles

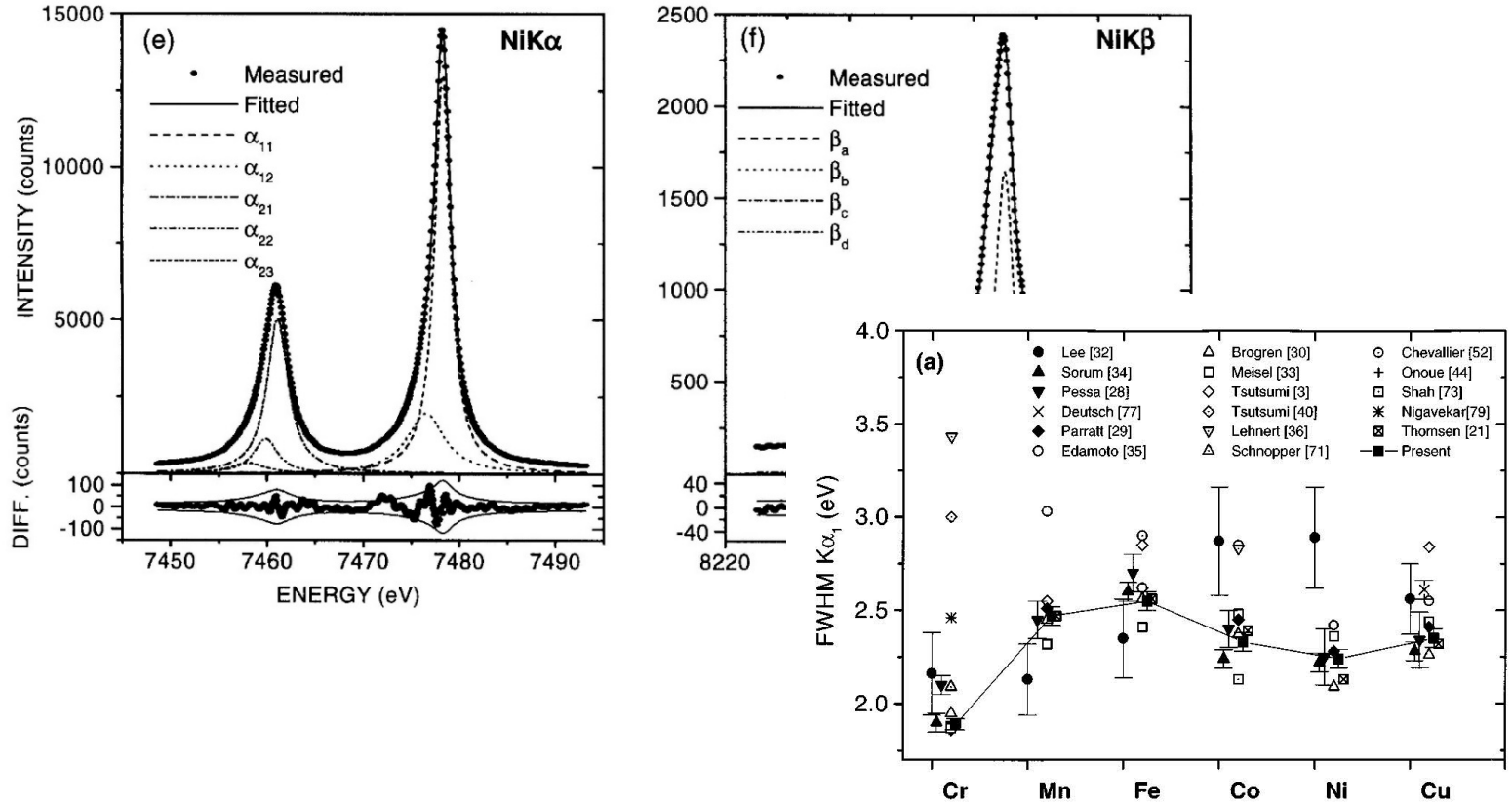

G. Hölzer, M. Fritsch, M. Deutsch, J. Härtwig, and E. Förster, "$K_{\alpha 1,2}$ and $K_{\beta 1,3}$ emission lines of *3d* transition metals", *Phys. Rev. A*, **56**, 4554-4568 (1997).

Multiconfiguration Dirac-Fock calculations in open-shell atoms: Convergence methods and satellite spectra of the copper Kα photoemission spectrum,
C. T. Chantler, J. A. Lowe, and I. P. Grant, Phys. Rev. A, 82, 052505 (2010).

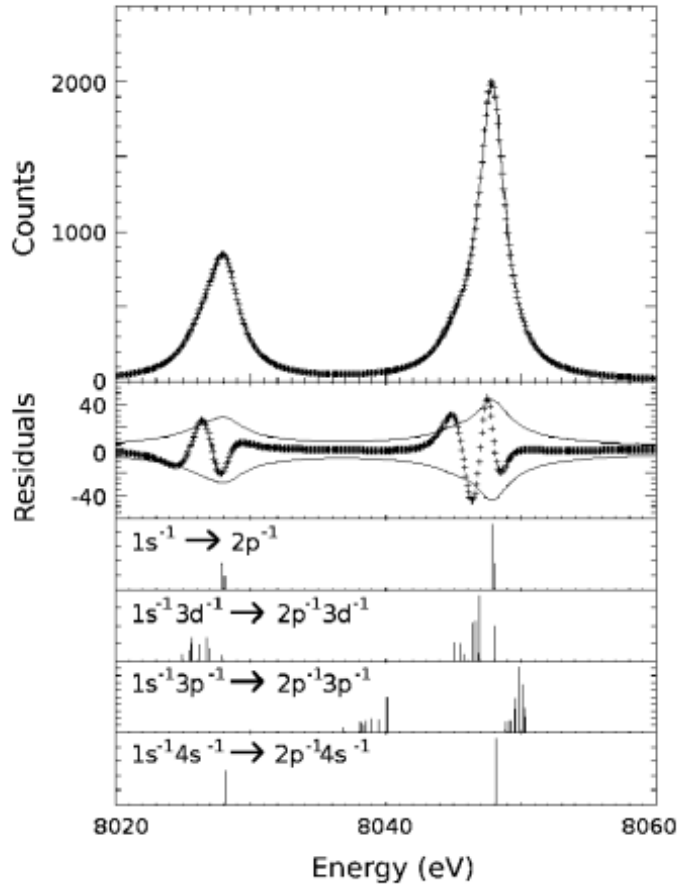

FIG. 1. Experimental and fitted theoretical spectrum for copper $K\alpha$. The curve bounding the residuals is $\pm\sigma$. The positions of the stick diagrams represent the transition energies contributing to the spectrum, and the height represents the intensity, normalized to the most intense transition of the group. The energy of the 4*s* spectator transition clearly indicates why approximate treatment of the open shell has provided good results in previous work.

High-precision measurement of the x-ray Cu Kα spectrum, M. H. Mendenhall, A. Henins, L. T. Hudson, C. I. Szabo, D. Windover, and J. P. Cline, *J. Phys. B: At. Mol. Opt. Phys.* **50**, 115004 (2017)

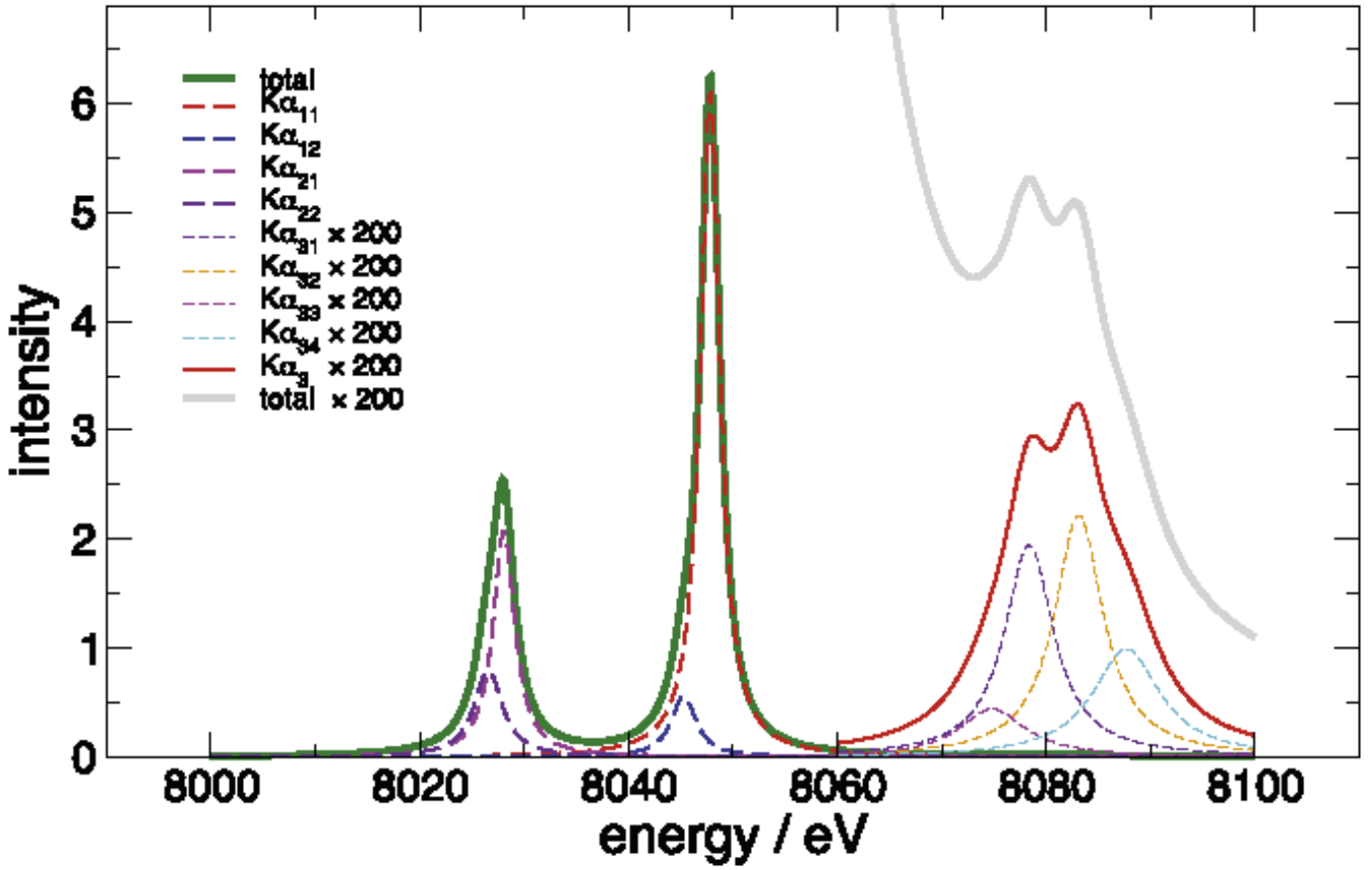

Figure 19. Separated peak components from the fit.

Hugo Rietveld's low-resolution neutron diffraction peaks were Gaussian (determined mainly by the neutron spectral distribution, the monochromator response function, and the divergences of the Soller collimators).
He used the "Caglioti" function to describe the widths.

H. M. Rietveld, "A Profile Refinement Method for Nuclear and Magnetic Strutcures", *J. Appl. Cryst*., **2**, 65-71 (1969).

G. Caglioti, A. Paoletti, and F. P. Ricci, "Choice of Collimators for a Crystal Spectrometer for Neutron Diffraction:,

Nucl. Inst., **3**, 223-228 (1958).

$$\mathrm{FWHM}^2 = U\tan^2\theta + V\tan\theta + W$$

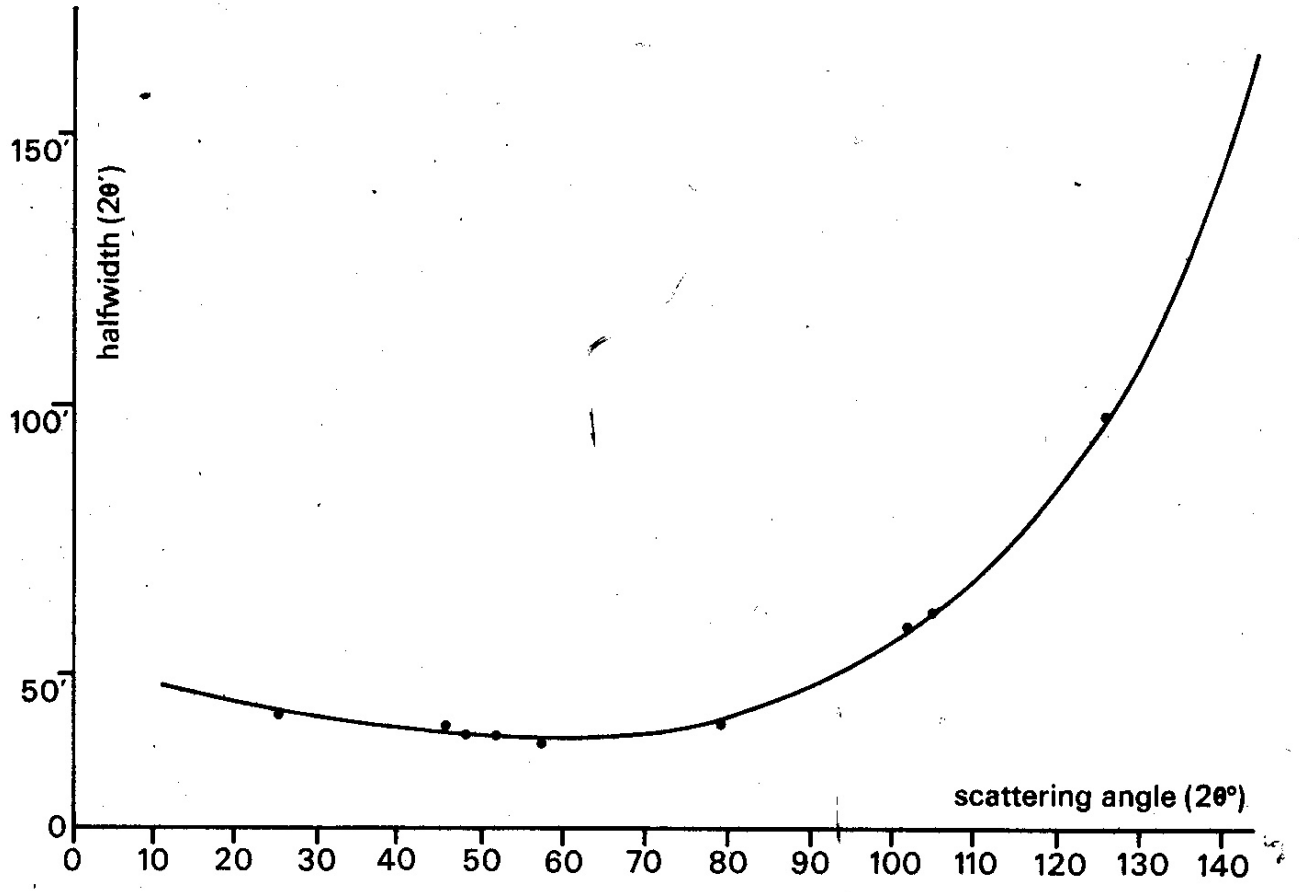

Fig. 3. Variation of peak width with Bragg angle; .... measured halfwidths, —— calculated curve.

$$\mathrm{FWHM}^2 = A\tan^2\theta + B\tan\theta + C + \mathrm{D}\cot^2\theta$$

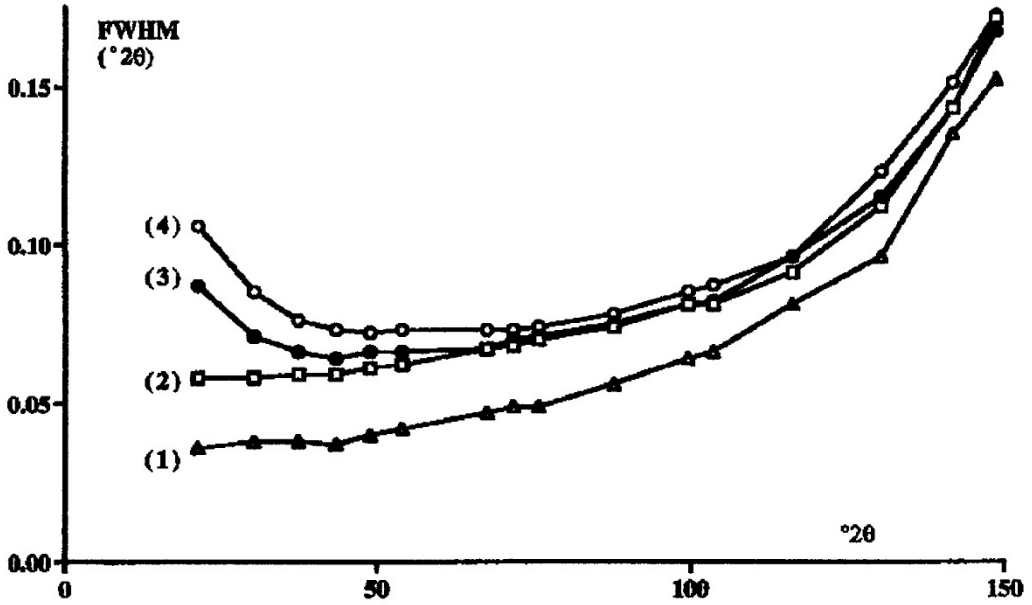

Fig. 3. FWHM curves for SRM 660 LaB_6 different slit configurations. Curve (1) corresponds to a receiving slit = 0.013°, a divergence slit of 0.25° and two Soller slits. Each curve corresponds to a change in one of the slits. Curve (1) to (2) is produced by an increase in receiving slit from 0.013° to 0.053°. Curve(2) to (3) arises from the increase in divergence slit from 0.25° to 1.25°. Curve (3) to (4) occurs when the diffracted beam Soller slit is removed. Error bars have been omitted because they are approximately the size of the plotted symbols.

R. W. Cheary and J. P. Cline, "An Analysis of the Effect of Different Instrumental Conditions on the Shapes of X-ray Powder Line Profiles", *Adv. X-ray Anal.,* **38**, 75-82 (1995).

Specimen Contributions

Size and (micro)Strain

Size Broadening

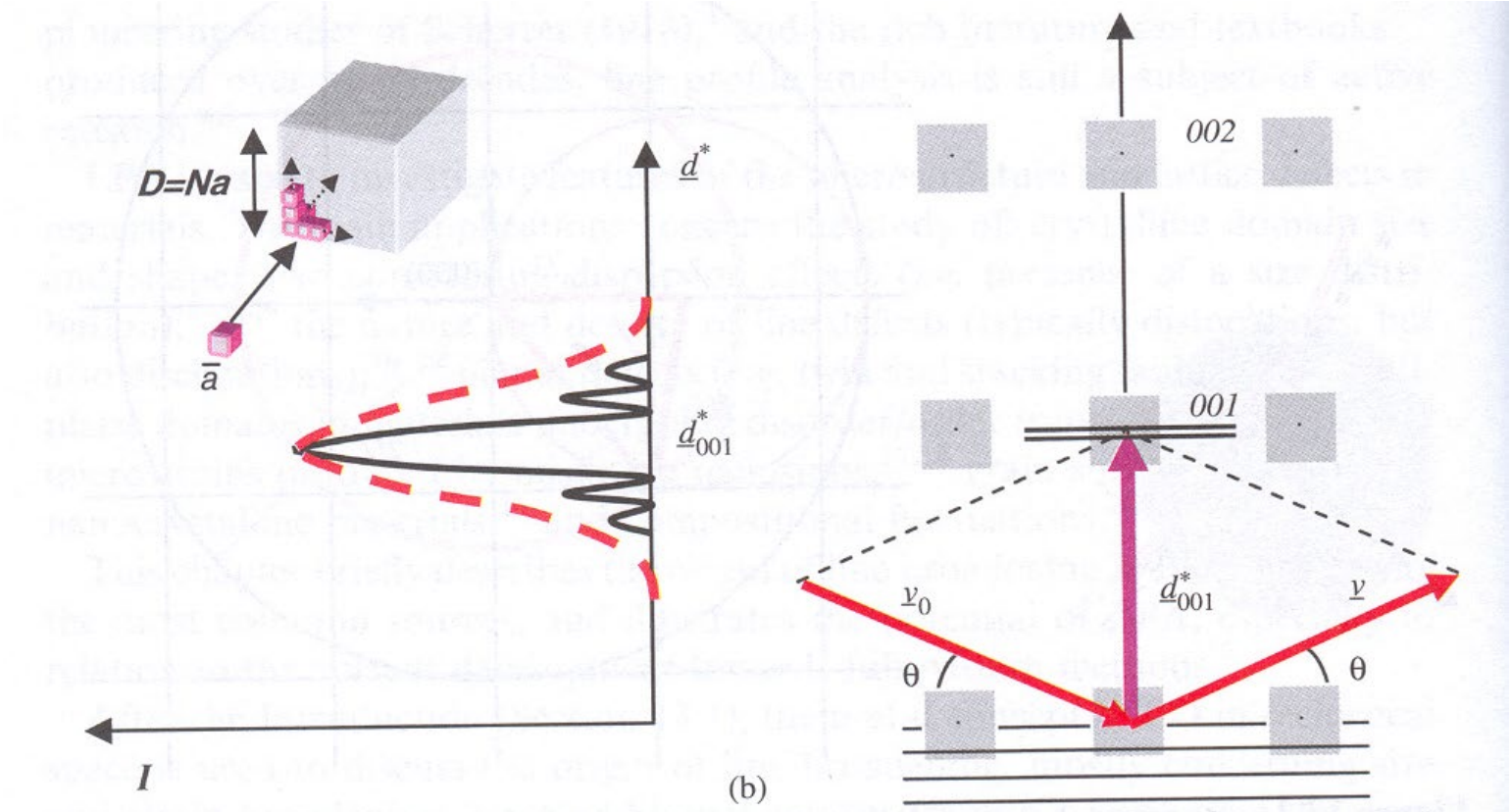

Figure 13.2 Schematic representation of the (001) diffraction condition (right) and amplitude of the diffracted intensity (left) in reciprocal space for an ideally perfect crystal (a) and for cubic crystalline domains of edge D [inset of (b)]. The profile for a dispersed system of cubic crystallites (dashed line) is also sketched out in (b).

P. Scardi, "Microstructural Properties: Lattice Defects and Domain Size Effects", in R. E. Dinnebier and S.J. L. Billinge, *Powder Diffraction: Theory and Practice*, RSC Publishing (2008)

Integral Breadth

$$\beta(s) = \frac{\int_{-\infty}^{\infty} I(s)ds}{I(0)} = \frac{\int_{-\infty}^{\infty} \frac{\sin^2(\pi Nas)}{(\pi as)^2} ds}{\underset{s\to 0}{Lim} \frac{\sin^2(\pi Nas)}{(\pi as)^2}} = \frac{Na}{(Na)^2} = \frac{1}{D}$$

Convert to 2θ space from reciprocal space:

$$\beta(2\theta) = \frac{\lambda K_\beta}{D\cos\theta}$$

Scherrer Constants for Various Crystallite Shapes

Shape	K (FWHM)	K (integral breadth)
Sphere	0.89	1.07
Cube	0.83-0.91	1.00-1.16
Tetrahedron	0.73-1.03	0.94-1.39
Octahedron	0.82-0.94	1.04-1.14

J. I. Langford and A. J. C. Wilson, “Scherrer after sixty years: A survey and some new results in the determination of crystallite size”, *J. Appl. Cryst.*, **11**, 102-113 (1978)

Shape?

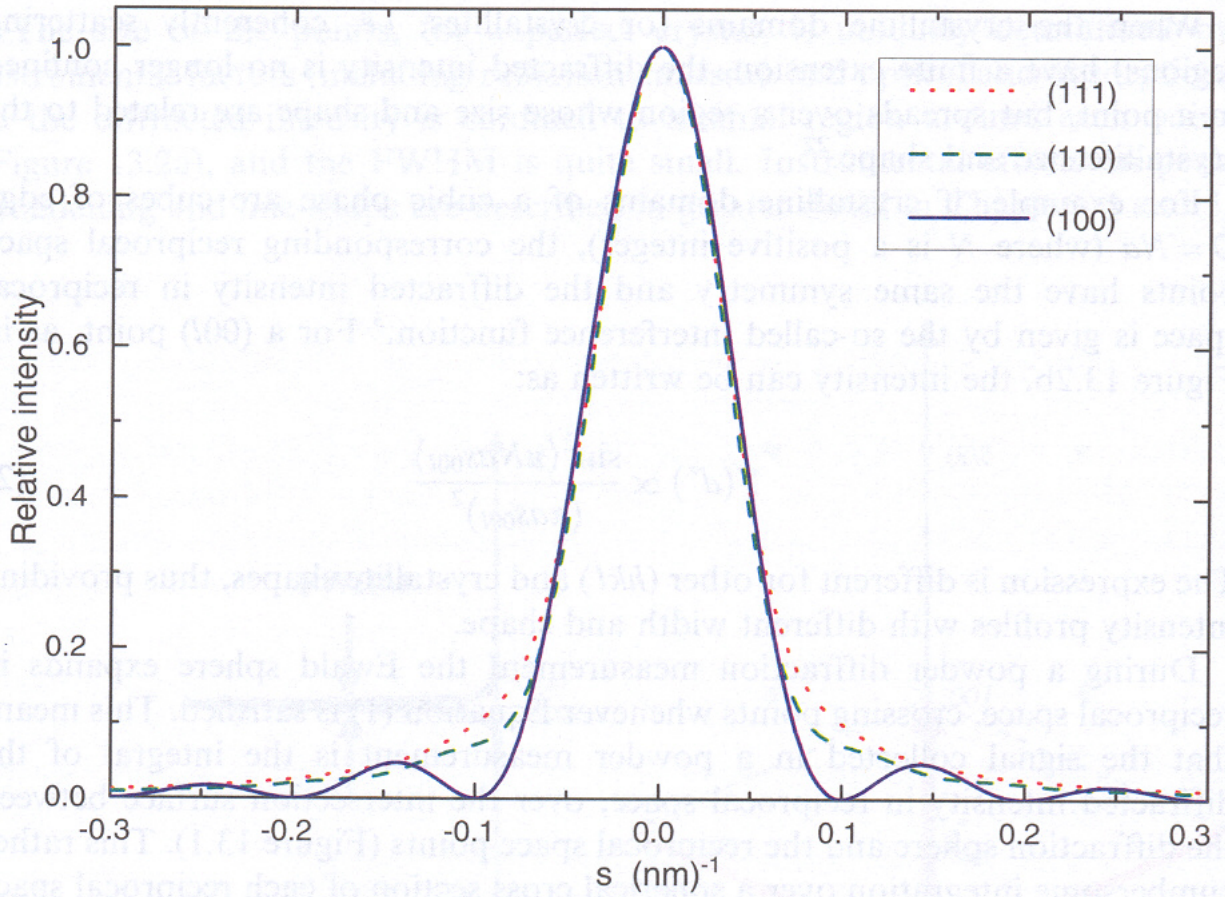

Figure 13.3 PD (100) (line), (110) (dash) and (111) (dot) peak profiles for a system made of cubic crystallites (edge $D = 10$ nm). Normalized profiles in reciprocal space.

P. Scardi, "Microstructural Properties: Lattice Defects and Domain Size Effects", in R. E. Dinnebier and S.J. L. Billinge, *Powder Diffraction: Theory and Practice*, RSC Publishing (2008)

P. Scardi and M. Leoni, "Diffraction line profiles from polydisperse crystalline systems", *Acta Cryst. Sect. A*, **57**, 604-613 (2001).

Size Distribution in Ceria Powder

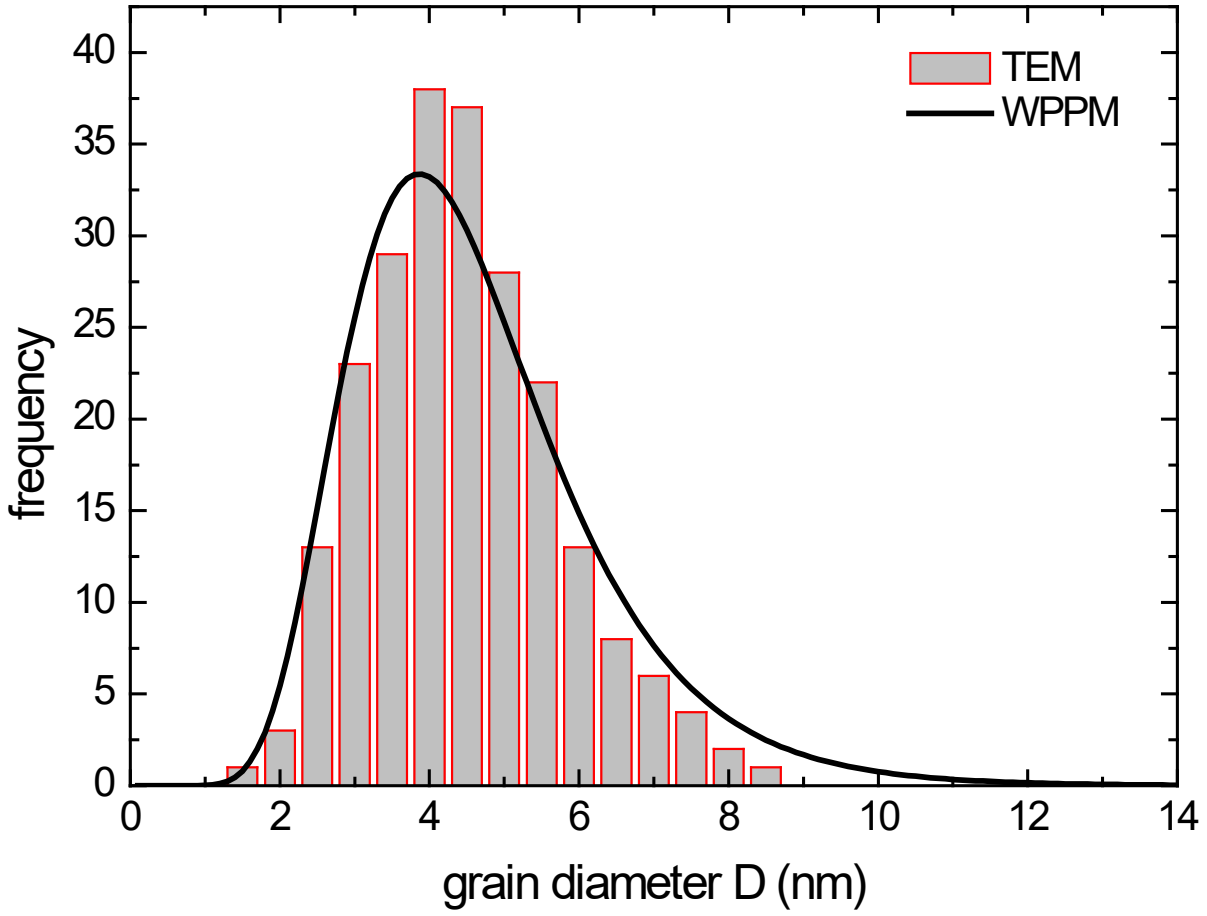

Strain Broadening

Macrostrain

$$\lambda = 2d \sin\theta$$

$$0 = 2dd \sin\theta + 2d \cos\theta d\theta$$

$$0 = 2\Delta d \sin\theta + 2d \cos\theta \Delta\theta$$

$$\Delta 2\theta = -2\frac{\Delta d}{d}\tan\theta = -2\varepsilon \tan\theta$$

Microstrain

$$\beta(2\theta) \propto \left\langle \varepsilon^2 \right\rangle^{1/2} \tan\theta$$

Microstrain

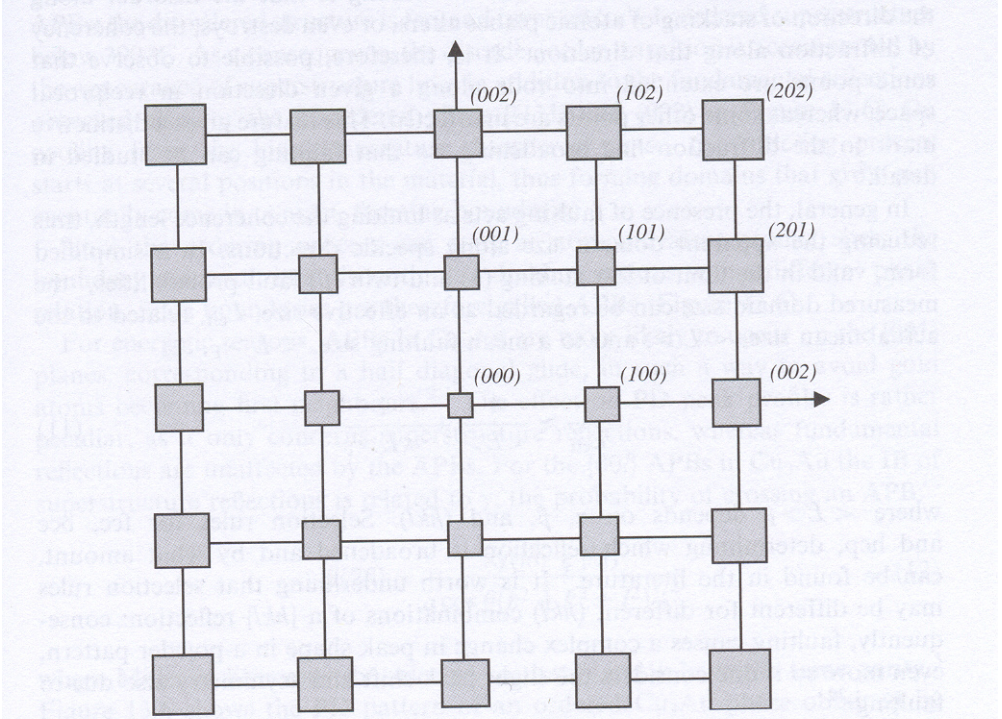

Figure 13.5 Strain broadening effect in reciprocal space. In this schematic picture, according to Equation (10), points spread increasingly with the distance from the origin.

P. Scardi, "Microstructural Properties: Lattice Defects and Domain Size Effects", in R. E. Dinnebier and S.J. L. Billinge, *Powder Diffraction: Theory and Practice*, RSC Publishing (2008)

Anisotropic Strain

P.W. Stephens, "Phenomenological model of anisotropic peak broadening in powder diffraction", *J. Appl. Cryst.*, **32**, 281-289 (1999)

$$\frac{1}{d^2} = M_{hkl} = Ah^2 + Bk^2 + Cl^2 + Dkl + Ehl + Fhk$$

$$\frac{1}{d^2} = M_{hkl} = \alpha_1 h^2 + \alpha_2 k^2 + \alpha_3 l^2 + \alpha_4 kl + \alpha_5 hl + \alpha_6 hk$$

$$\sigma^2(M_{hkl}) = \sum_{i,j} C_{ij} \frac{\partial M}{\partial \alpha_i} \frac{\partial M}{\partial \alpha_j}$$

$$\sigma^2(M_{hkl}) = \sum_{HKL} S_{HKL} h^H k^K l^L$$

$$H + K + L = 4$$

$$\sigma^2(M_{hkl}) = S_{400}h^4 + S_{040}k^4 + S_{004}l^4 + 3(S_{220}h^2k^2$$
$$+ S_{202}h^2l^2 + S_{022}k^2l^2) + 2(S_{310}h^3k + S_{103}hl^3$$
$$+ S_{031}k^3l + S_{130}hk^3 + S_{301}h^3l + S_{013}kl^3)$$
$$+ 3(S_{211}h^2kl + S_{121}hk^2l + S_{112}hkl^2)$$

Functional Forms of Size and Strain Broadening

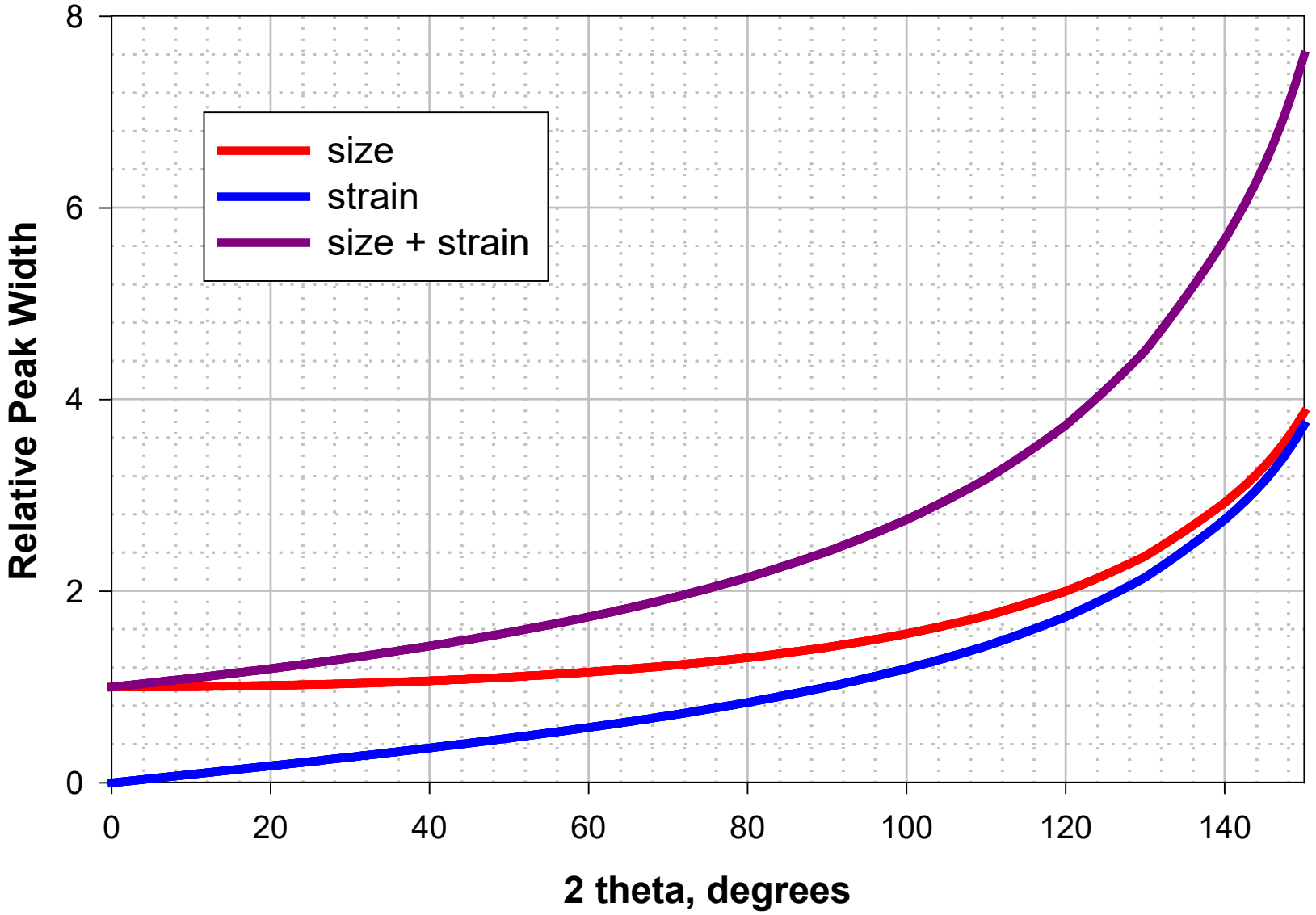

Williamson-Hall Analysis

Real peaks have both Gaussian and Lorentzian (Cauchy) components

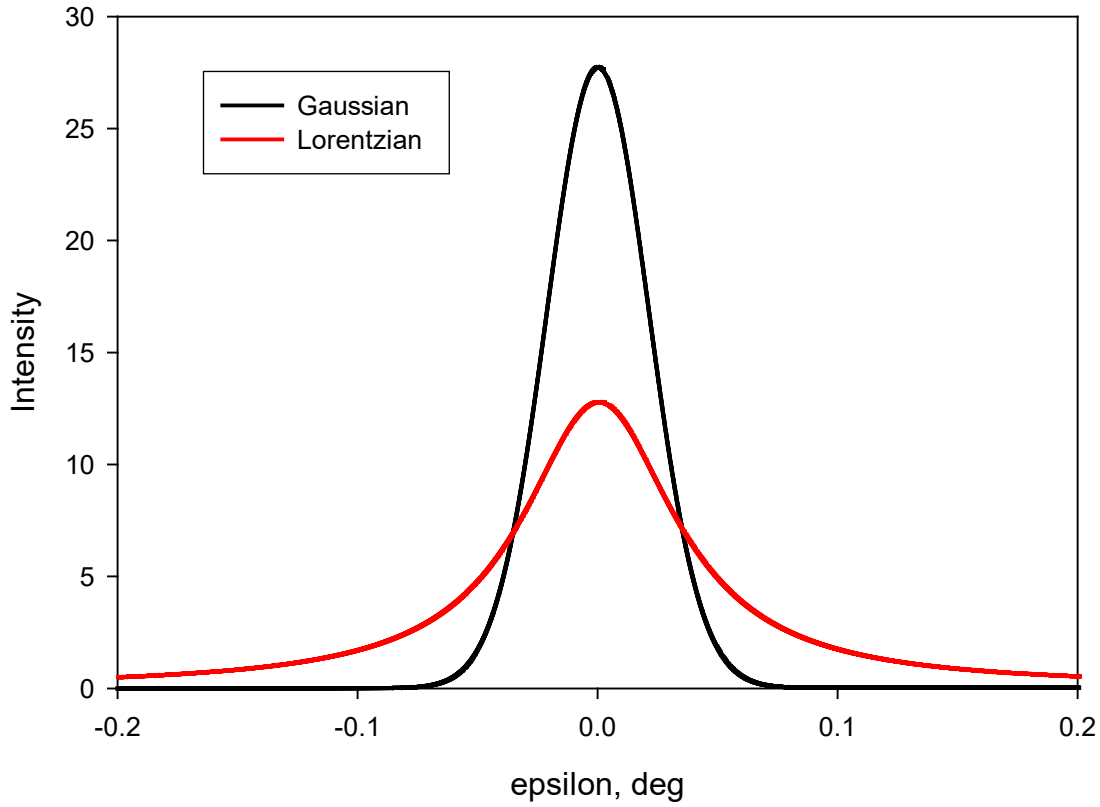

Same FWHM and area!

Profile Equations

Gaussian

$$I_{i,k} = \frac{2\sqrt{\ln 2}}{H_k} \exp\left[\frac{-4\ln 2}{H_k^2}\varepsilon^2\right]$$

Lorentzian

$$I_{i,k} = \frac{2}{\pi H_k}\left[1 + \frac{4(\sqrt{2}-1)}{H_k^2}\varepsilon^2\right]^{-1}$$

S. A. Howard and K. D. Preston, “Profile Fitting of Powder Diffraction Patterns”, in D. L. Bish and J. E. Post, *Modern Powder Diffraction* (1989), p. 217-275.

SRM 660a LaB_6

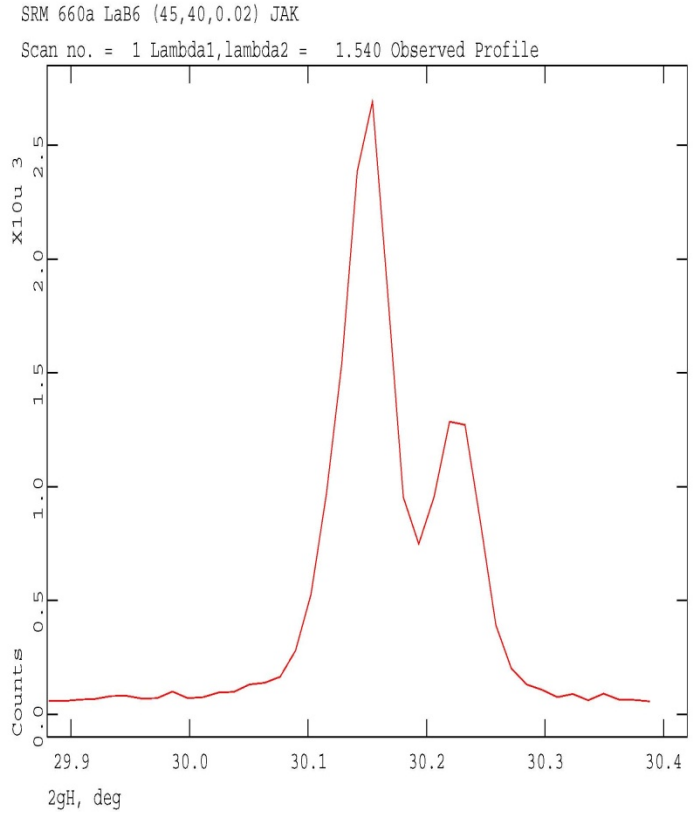

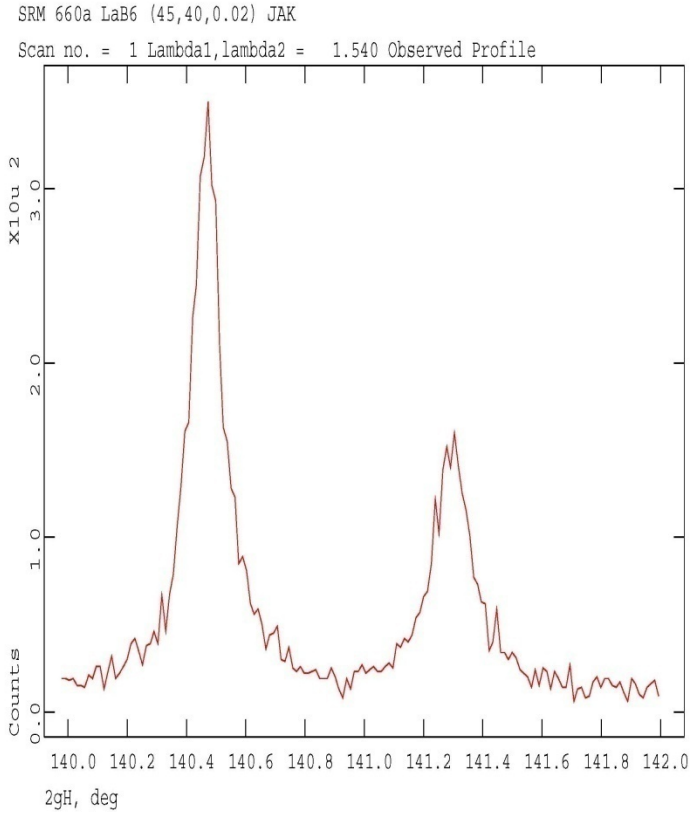

So use combination of Gaussian and Lorentzian

Voigt (convolution)

pseudo-Voigt (sum)

L. W. Finger, D. E. Cox, and A. P. Jephcoat, “A Correction for Powder Diffraction Peak Asymmetry due to Axial Divergence”,
J. Appl. Cryst., **27**, 892-900 (1994).

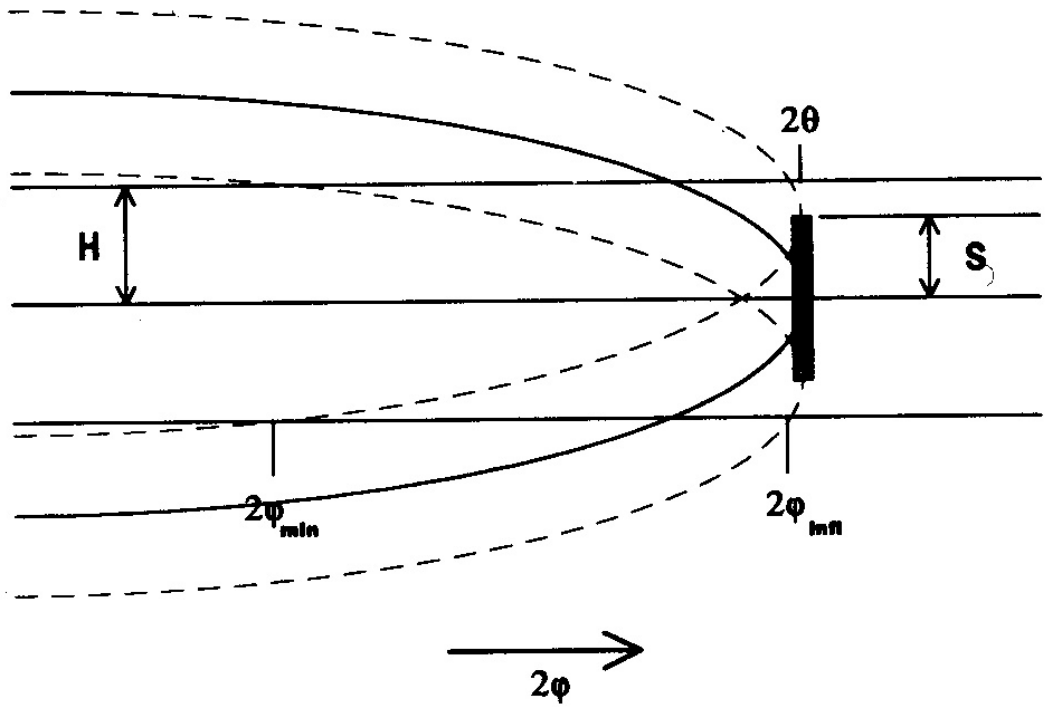

Fig. 1. The band of intensity, diffracted by a sample with height $2S$, as seen by a detector with opening $2H$ and a detector angle 2φ moving in the detector cylinder. The figure is adapted from that of van Laar & Yelon (1984). For angles below $2\varphi_{\min}$, no intensity is seen. For angles between $2\varphi_{\text{infl}}$ and 2θ, the entire sample can be seen by the detector.

GSAS-I Profile Functions #3-5

S/L = sample “half height”/diffractometer radius
H/L = slit “half height”/diffractometer radius
6/240 = 0.025

GSAS-I Profile Function #2 (3-5)
Thompson-Cox-Hastings pseudo-Voigt

$$\sigma^2 = GU\tan^2\theta + GV\tan\theta + GW + \frac{GP}{\cos^2\theta}$$

$$\gamma = \frac{LX + ptec\cos\varphi}{\cos\theta} + \left(LY + stec\cos\varphi\right)\tan\theta$$

$$\Delta 2\theta = zero + \left(\frac{f_i asym}{\tan 2\theta}\right) + shft\cos\theta + trns\sin 2\theta$$

NIST SRM 660c LaB_6

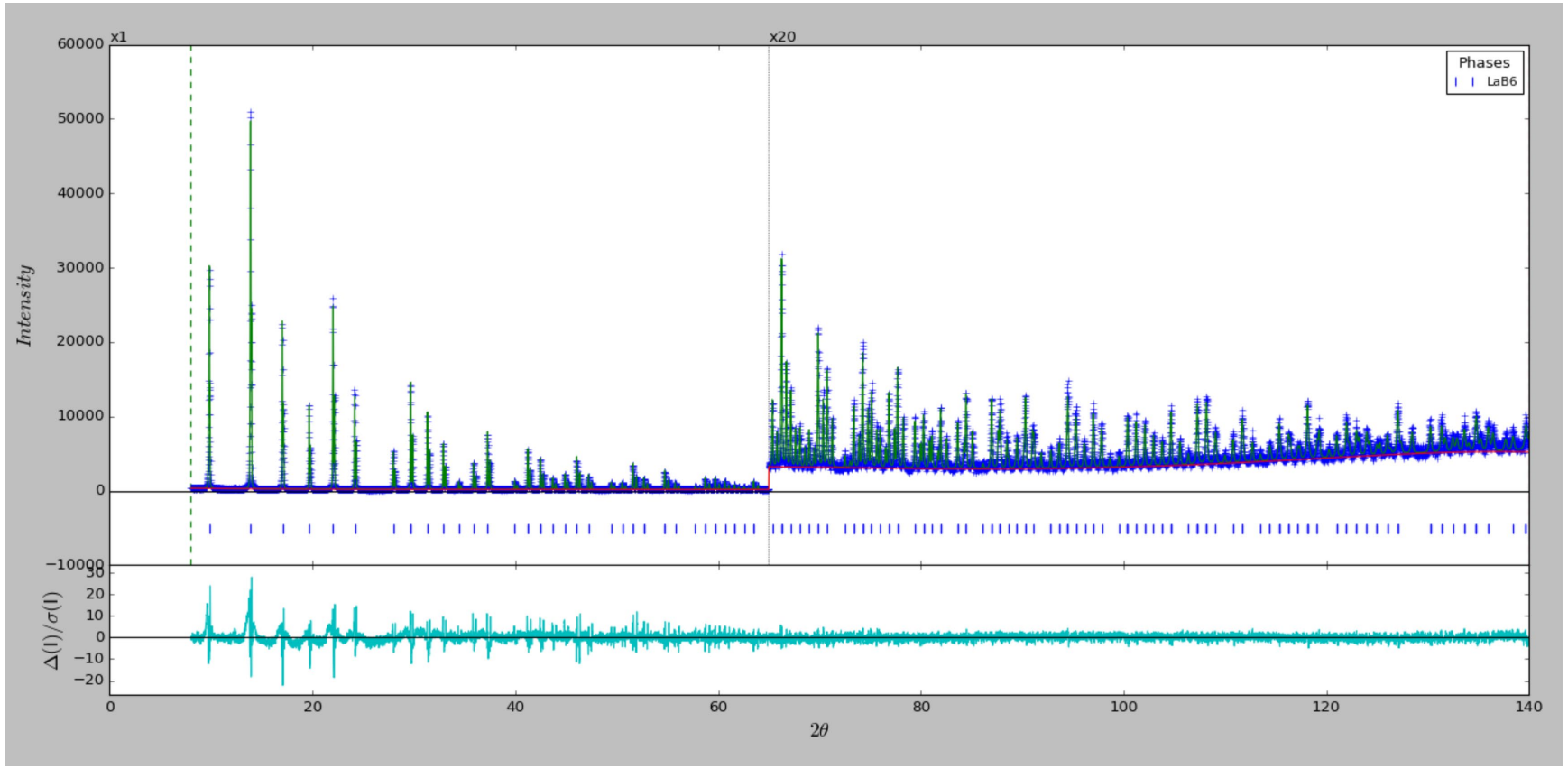

GSAS-II

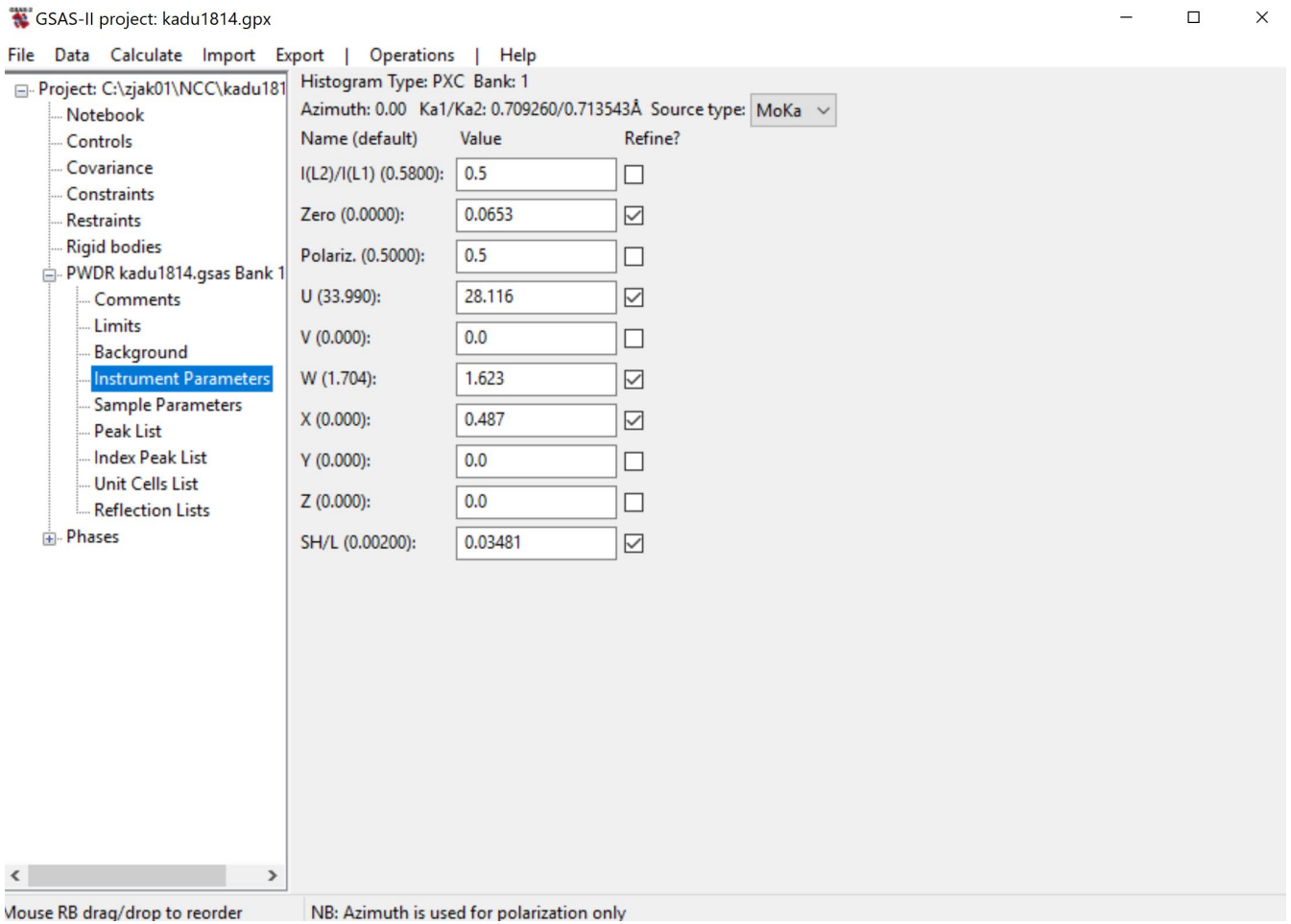
GSAS-II project: kadu1814.gpx
File Data Calculate Import Export | Operations | Help
Project: C:\zjak01\NCC\kadu181
Notebook
Controls
Covariance
Constraints
Restraints
Rigid bodies
PWDR kadu1814.gsas Bank 1
Comments
Limits
Background
Instrument Parameters
Sample Parameters
Peak List
Index Peak List
Unit Cells List
Reflection Lists
Phases
Histogram Type: PXC Bank: 1
Azimuth: 0.00 Ka1/Ka2: 0.709260/0.713543Å Source type: MoKa
Name (default) Value Refine?
I(L2)/I(L1) (0.5800): 0.5
Zero (0.0000): 0.0653
Polariz. (0.5000): 0.5
U (33.990): 28.116
V (0.000): 0.0
W (1.704): 1.623
X (0.000): 0.487
Y (0.000): 0.0
Z (0.000): 0.0
SH/L (0.00200): 0.03481
Mouse RB drag/drop to reorder
NB: Azimuth is used for polarization only

GSAS-II Instrument Parameter File

PANalytical Empyrean/Mo/capillary

```
#GSAS-II instrument parameter file; do not add/delete items!
I(L2)/I(L1):0.5
SH/L:0.0348141083102
Azimuth:0.0
Lam2:0.713543
Source:MoKa
Zero:0.0652623352976
Lam1:0.70926
U:28.1161839663
W:1.62280279963
V:0.0
Y:0.0
X:0.486972245354
Z:0.0
Type:PXC
Bank:1
Polariz.:0.5
```

GSAS-II Phase Data

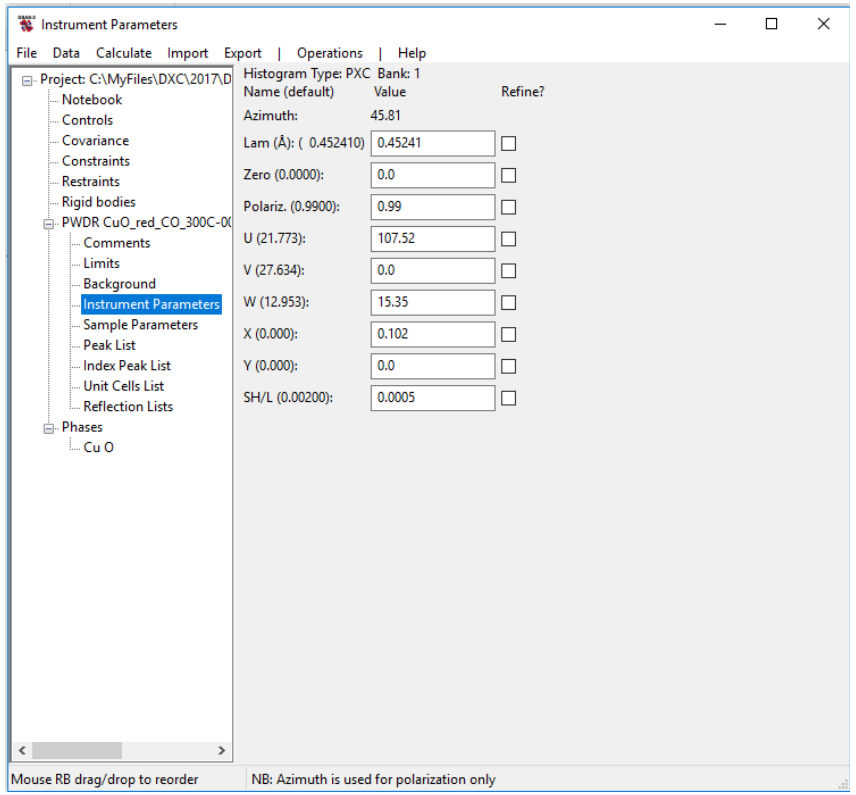

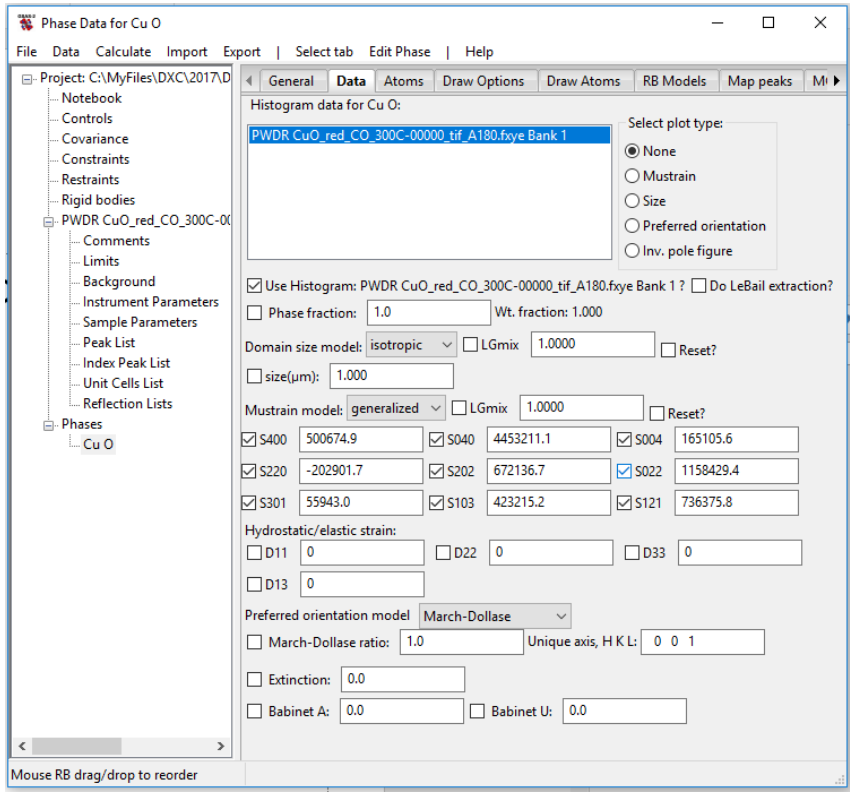

Control of Peak Positions

- Lattice parameters
- Specimen displacement
- Specimen transparency
- (Zero)

Specimen Displacement (GSAS-I)

$$\Delta 2\theta = shft \cos\theta$$

$$s = \frac{-\pi R shft}{36000}$$

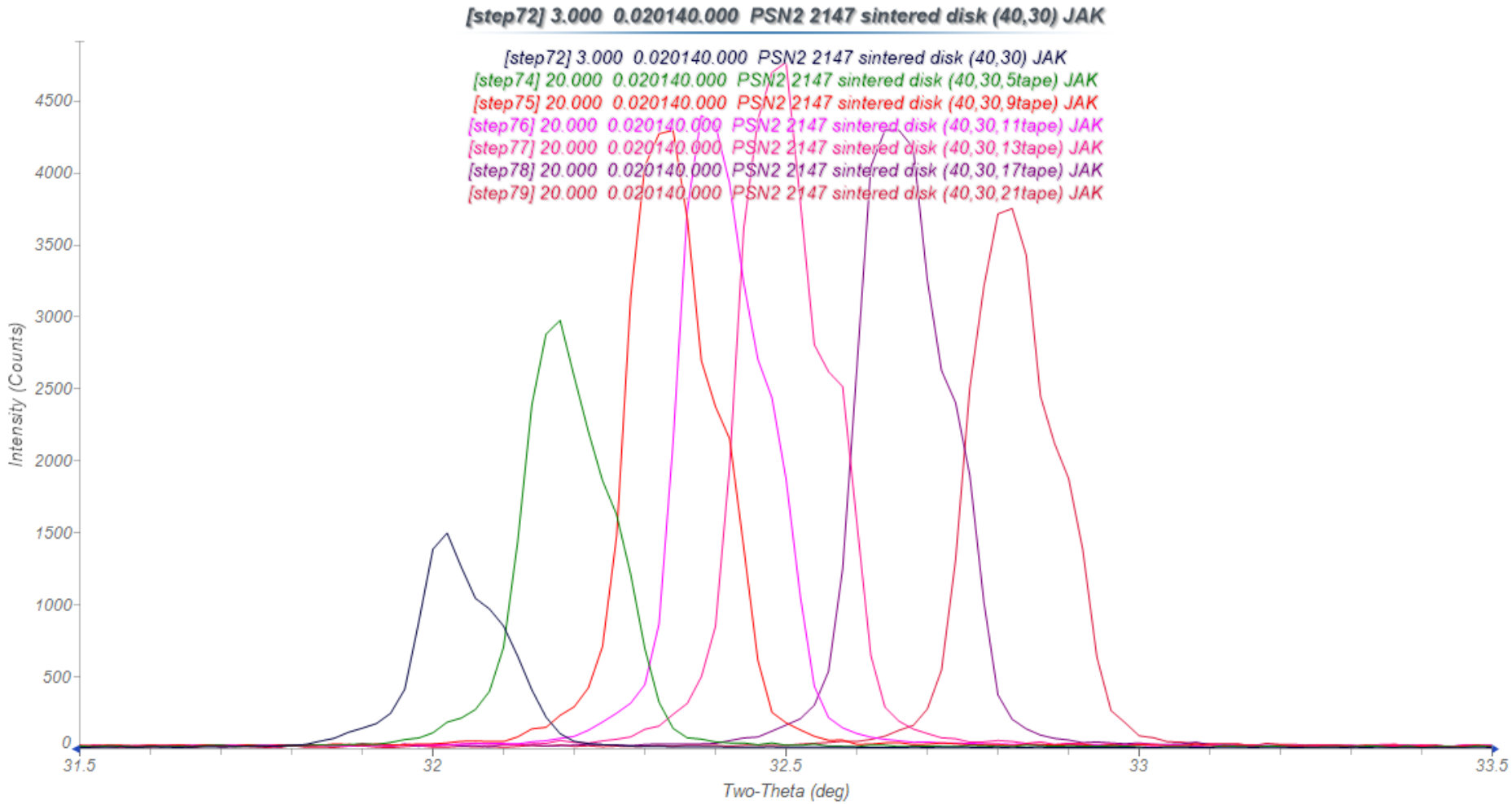
[step72] 3.000 0.020140.000 PSN2 2147 sintered disk (40,30) JAK
[step72] 3.000 0.020140.000 PSN2 2147 sintered disk (40,30) JAK
[step74] 20.000 0.020140.000 PSN2 2147 sintered disk (40,30,5tape) JAK
[step75] 20.000 0.020140.000 PSN2 2147 sintered disk (40,30,9tape) JAK
[step76] 20.000 0.020140.000 PSN2 2147 sintered disk (40,30,11tape) JAK
[step77] 20.000 0.020140.000 PSN2 2147 sintered disk (40,30,13tape) JAK
[step78] 20.000 0.020140.000 PSN2 2147 sintered disk (40,30,17tape) JAK
[step79] 20.000 0.020140.000 PSN2 2147 sintered disk (40,30,21tape) JAK
Intensity (Counts)
4500
4000
3500
3000
2500
2000
1500
1000
500
0
31.5
32
32.5
33
33.5
Two-Theta (deg)

Measured and Calculated Specimen Displacements
PSN2 2147

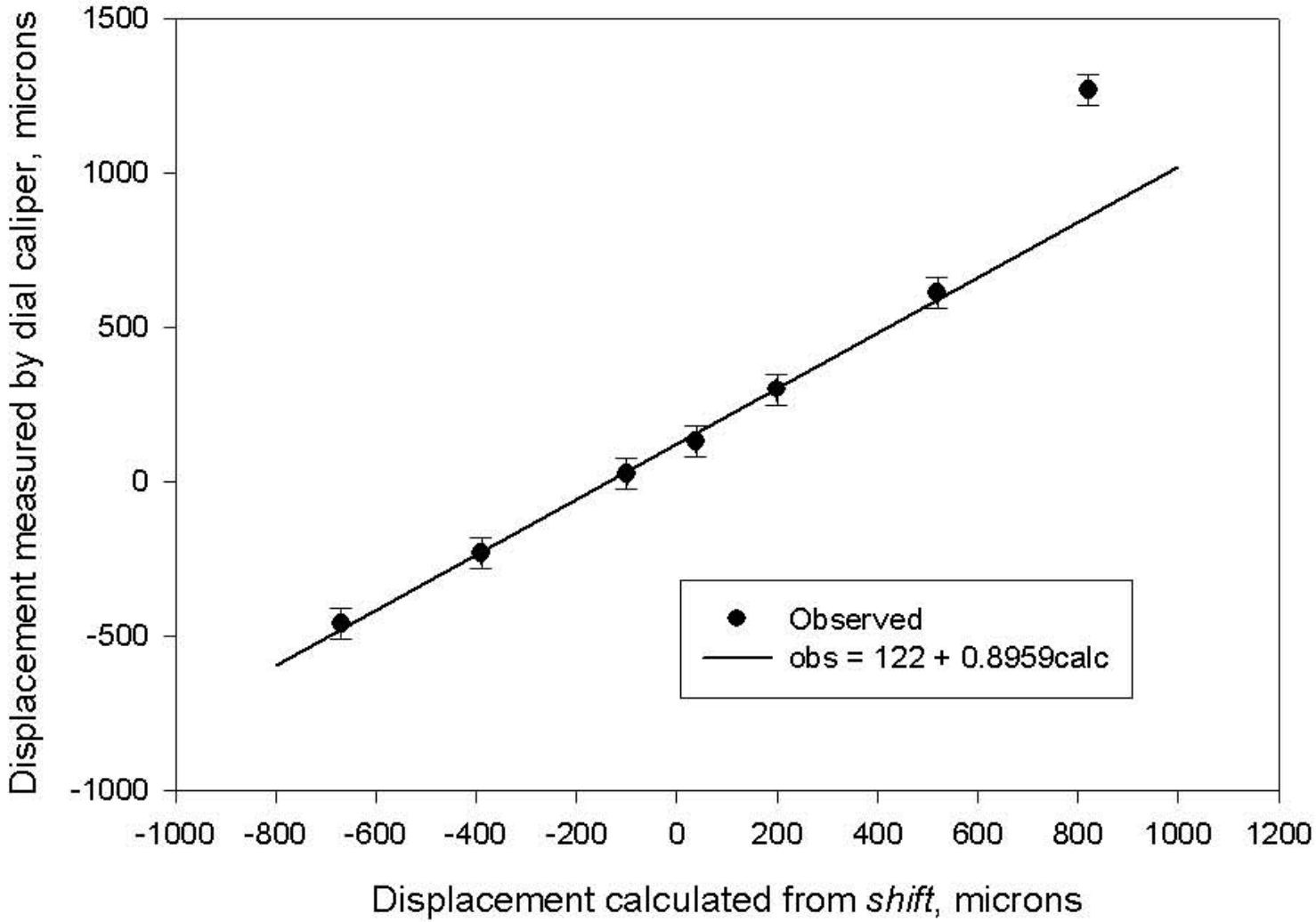

Specimen Displacement

Displacement, μm	*shift*	*a*, Å
-670	36.79(3)	3.90997(2)
-390	21.25(5)	3.91010(2)
-100	5.56(4)	3.91016(2)
38	-2.06(3)	3.91025(1)
200	-10.78(4)	3.91007(2)
520	-28.57(4)	3.91025(2)
820	-44.75(5)	3.91025(2)
Average		3.9102(1)

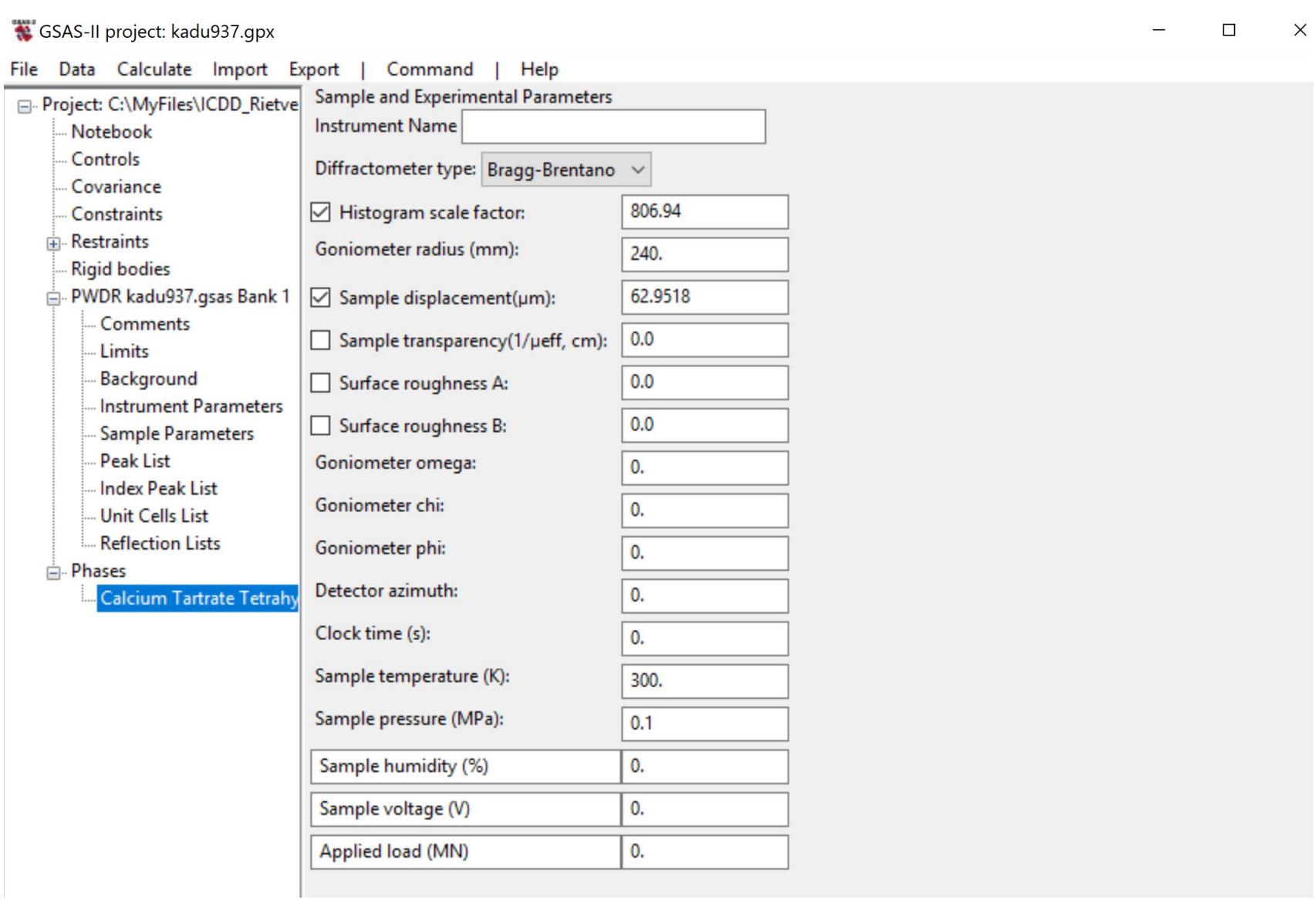
GSAS-II project: kadu937.gpx
File
Data
Calculate
Import
Export
Command
Help
Project: C:\MyFiles\ICDD_Rietve
Notebook
Controls
Covariance
Constraints
Restraints
Rigid bodies
PWDR kadu937.gsas Bank 1
Comments
Limits
Background
Instrument Parameters
Sample Parameters
Peak List
Index Peak List
Unit Cells List
Reflection Lists
Phases
Calcium Tartrate Tetrahy
Sample and Experimental Parameters
Instrument Name
Diffractometer type: Bragg-Brentano
Histogram scale factor: 806.94
Goniometer radius (mm): 240.
Sample displacement(μm): 62.9518
Sample transparency(1/μeff, cm): 0.0
Surface roughness A: 0.0
Surface roughness B: 0.0
Goniometer omega: 0.
Goniometer chi: 0.
Goniometer phi: 0.
Detector azimuth: 0.
Clock time (s): 0.
Sample temperature (K): 300.
Sample pressure (MPa): 0.1
Sample humidity (%) 0.
Sample voltage (V) 0.
Applied load (MN) 0.

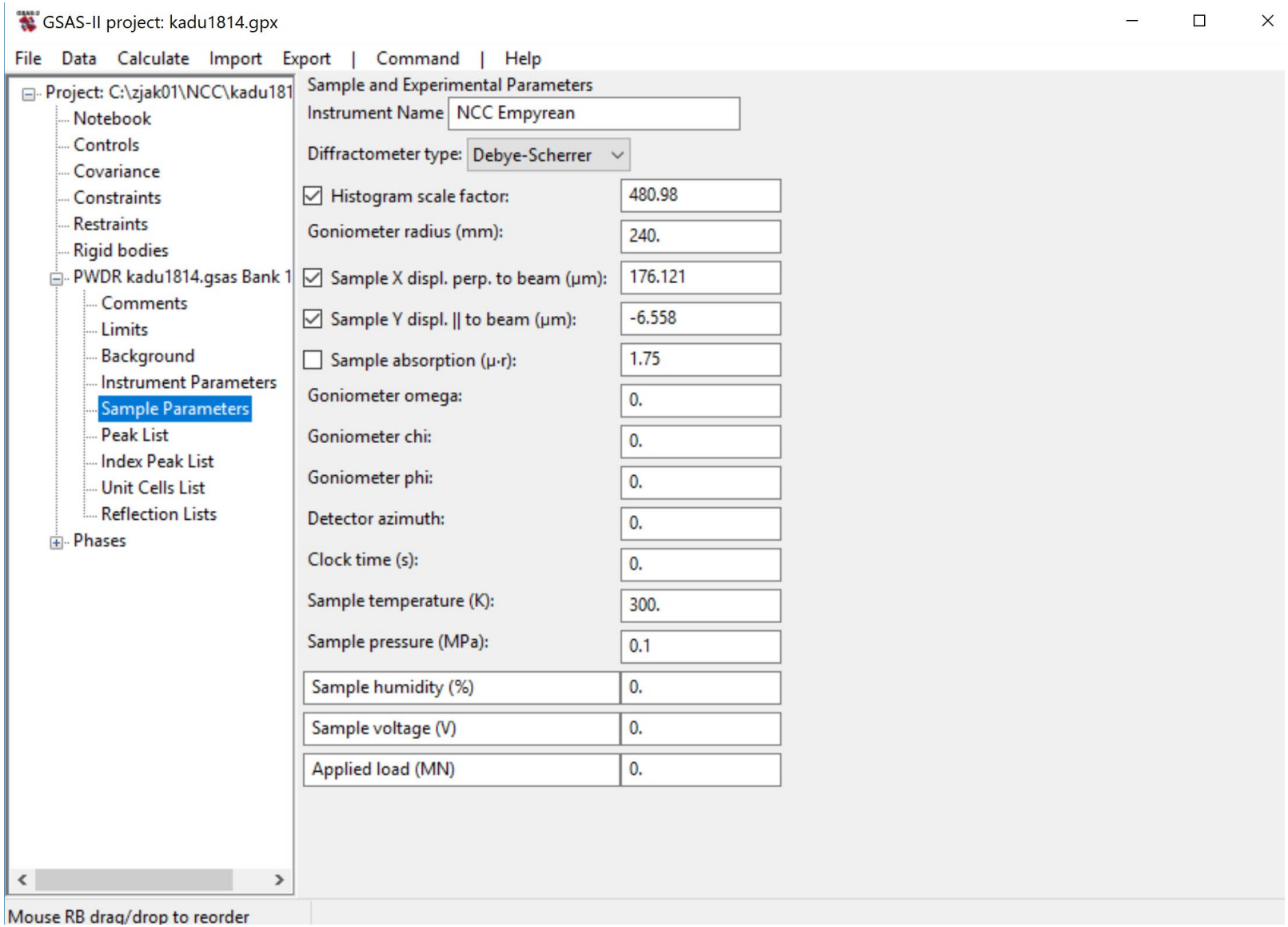
GSAS-II project: kadu1814.gpx
File Data Calculate Import Export | Command | Help
Project: C:\zjak01\NCC\kadu181
Notebook
Controls
Covariance
Constraints
Restraints
Rigid bodies
PWDR kadu1814.gsas Bank 1
Comments
Limits
Background
Instrument Parameters
Sample Parameters
Peak List
Index Peak List
Unit Cells List
Reflection Lists
Phases
Sample and Experimental Parameters
Instrument Name NCC Empyrean
Diffractometer type: Debye-Scherrer
Histogram scale factor: 480.98
Goniometer radius (mm): 240.
Sample X displ. perp. to beam (μm): 176.121
Sample Y displ. || to beam (μm): -6.558
Sample absorption (μ·r): 1.75
Goniometer omega: 0.
Goniometer chi: 0.
Goniometer phi: 0.
Detector azimuth: 0.
Clock time (s): 0.
Sample temperature (K): 300.
Sample pressure (MPa): 0.1
Sample humidity (%) 0.
Sample voltage (V) 0.
Applied load (MN) 0.
Mouse RB drag/drop to reorder

Specimen Transparency

When the specimen is long enough to intercept the whole beam, and

$$t \geq \frac{3.2}{\mu}\frac{\rho}{\rho'}\sin\theta$$

an additional component of the profile g is generated:

$$g = \exp\left(\frac{4\pi R\varepsilon}{114.6}\sin 2\theta\right)$$

$$-\infty < \varepsilon \leq 0\ (^\circ)$$

Transparency

- Significant for thick organic specimens
- Additional low-angle asymmetry
- Peak shift to low angles

Extra Low-Angle Asymmetry
Peak Shift to Low-Angles

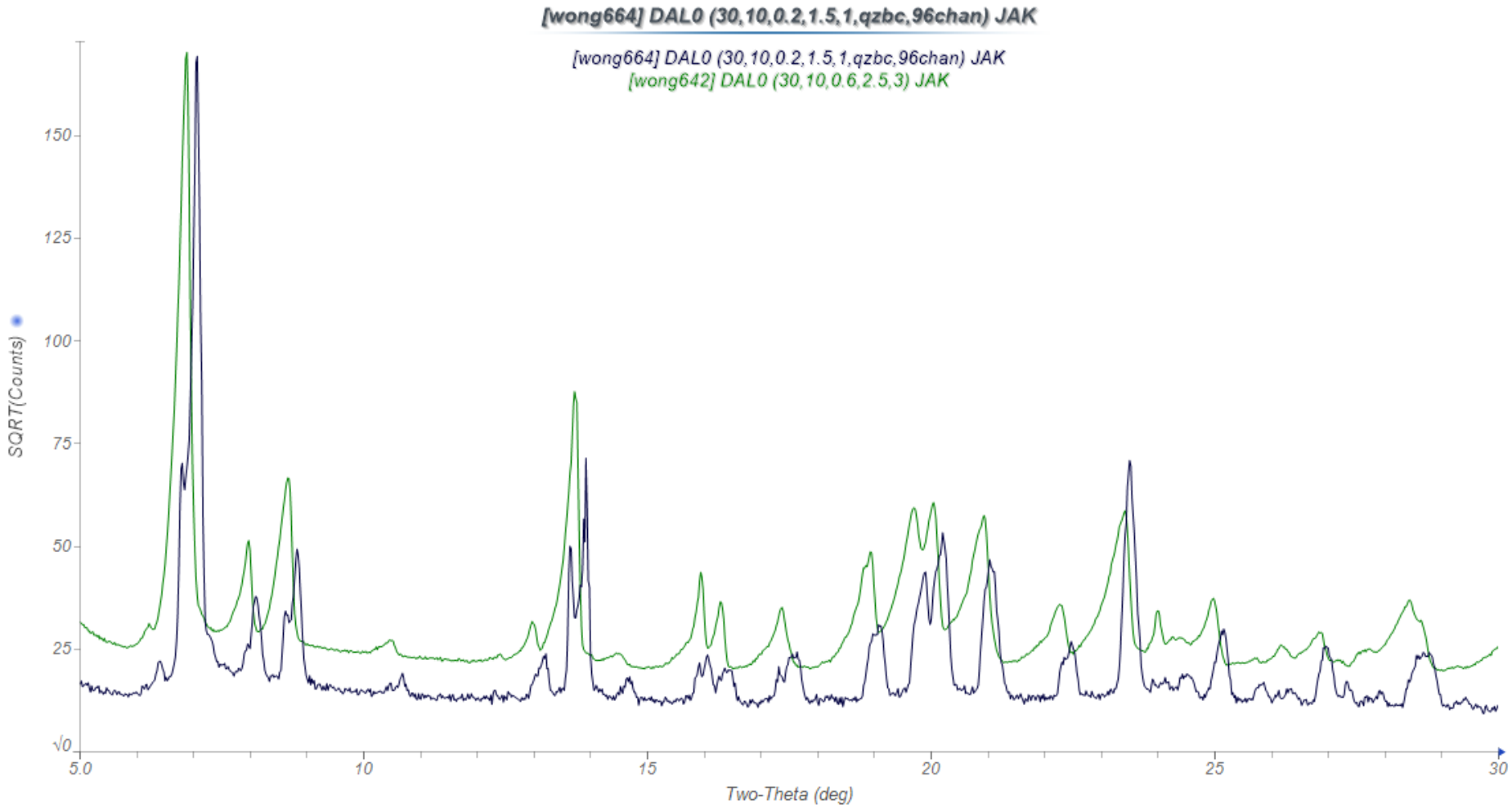

Specimen Transparency
GSAS-I

$$\Delta 2\theta = trns \sin 2\theta$$

$$\mu_{eff} = \frac{-9000}{\pi R trns}$$

10% RuO_2/SiO_2 Catalyst

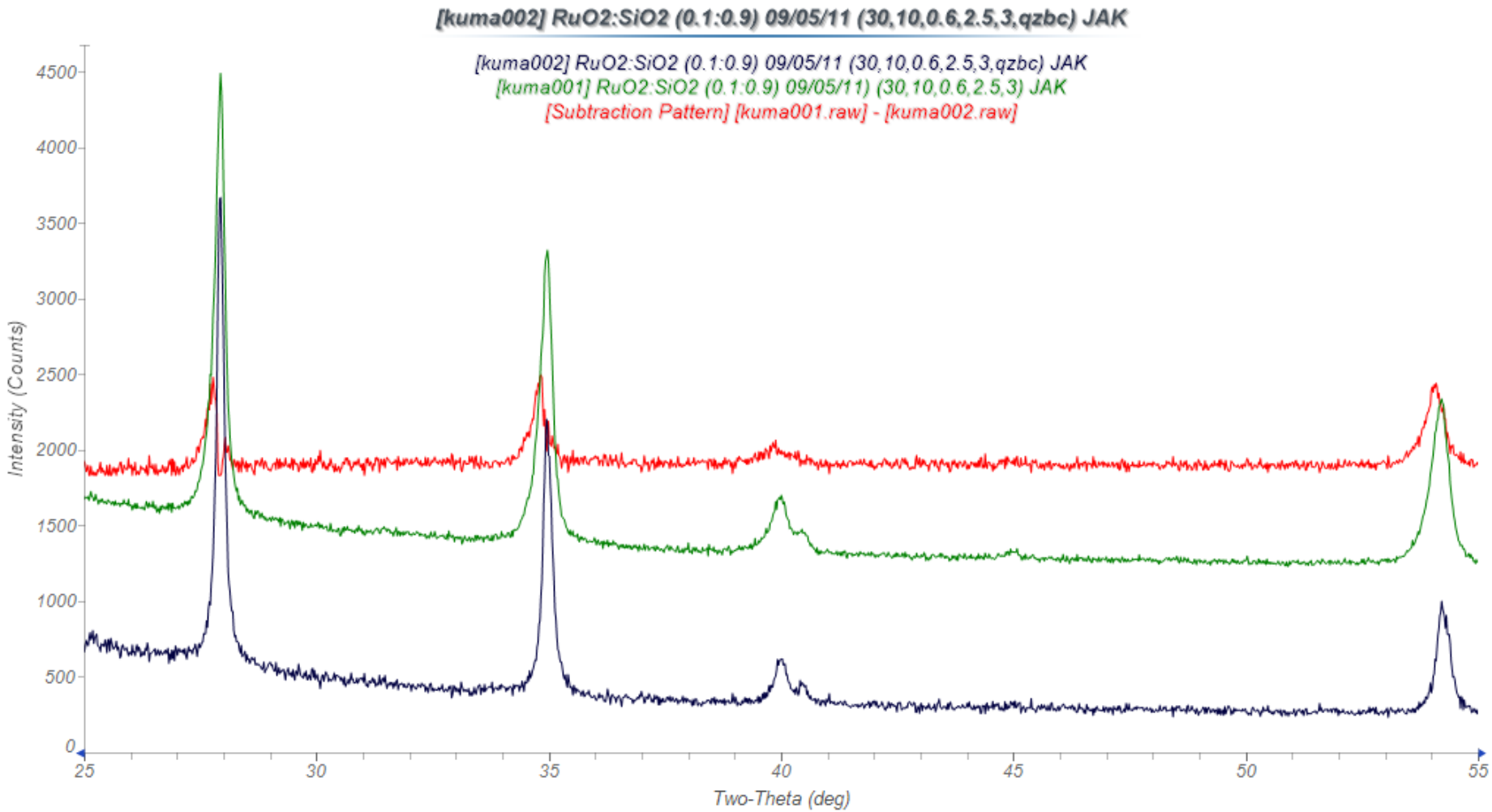

Penetration Depth, μm

2θ, °	28	130
Pure RuO_2	22	70
10% RuO_2/90% SiO_2	100	340

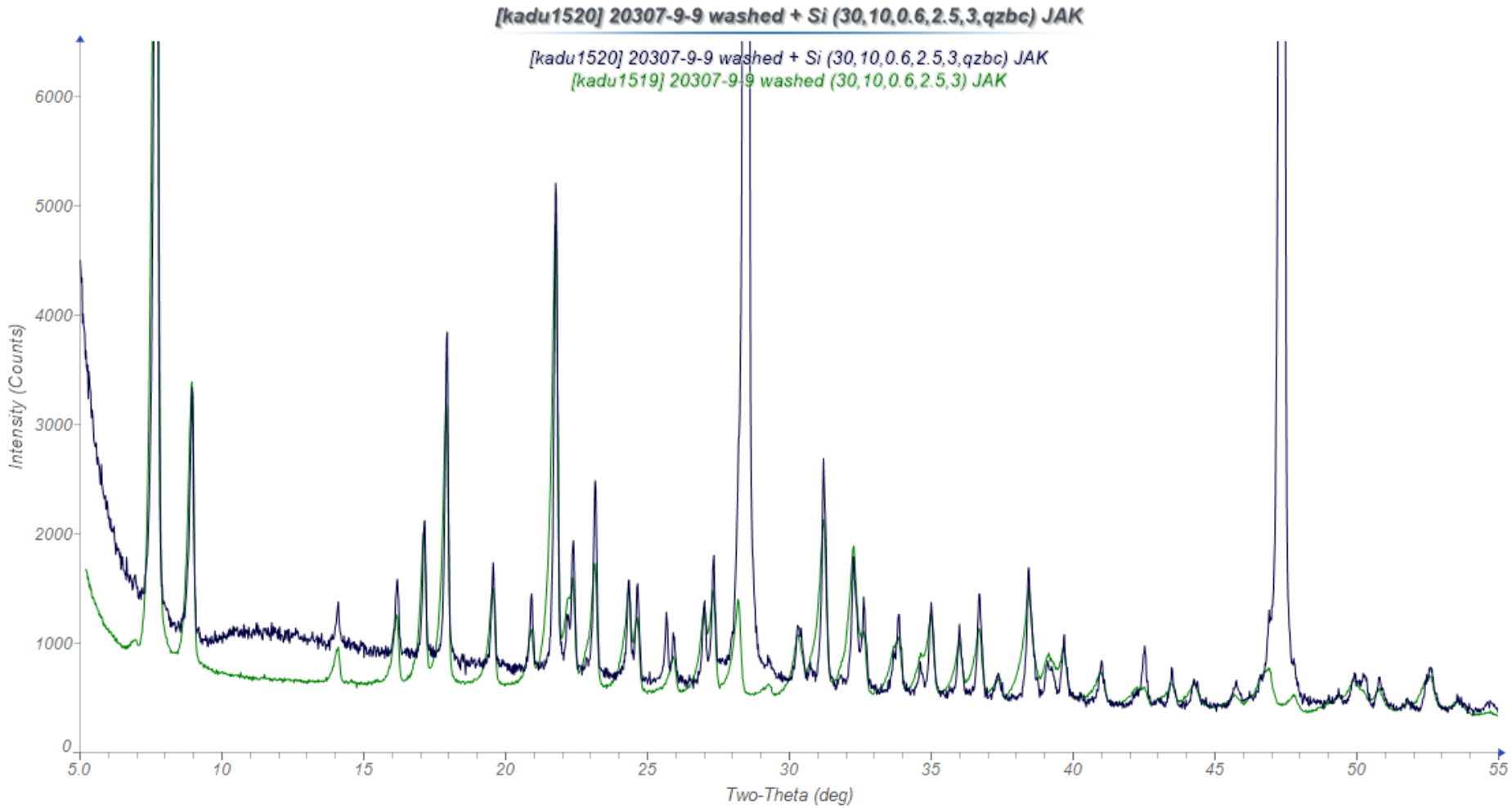
[kadu1520] 20307-9-9 washed + Si (30,10,0.6,2.5,3,qzbc) JAK
[kadu1520] 20307-9-9 washed + Si (30,10,0.6,2.5,3,qzbc) JAK
[kadu1519] 20307-9-9 washed (30,10,0.6,2.5,3) JAK
Intensity (Counts)
0
1000
2000
3000
4000
5000
6000
5.0
10
15
20
25
30
35
40
45
50
55
Two-Theta (deg)

Instrument Profiles

"Typical values of Rietveld instrument profile coefficients",

J. A. Kaduk and J. Reid, *Powder Diffraction,* **26**(1), 88-93 (2011).

Table II. GSAS Function #2 Instrument Profile Parameters for a Variety of Laboratory Diffractometers.

Diffractometer	Date	*U*	*V*	*W*	*X*	*Y*	*asym*
X'Pert Pro PIXcel/0.04 rad Soller	08/2010	0.8048	0	0.5103	2.537	1.946	4.343
D2/Lynxeye	05/2010	1.371	0	2.393	2.183	1.199	2.774
D2/Lynxeye	10/2009	2.8329	0	2.695	1.853	2.488	2.194
X'Pert Pro PIXcel/mono	01/2008	0.7565	0	3.646	2.428	1.902	1.063
X'Pert Pro PIXcel/no mon	01/2008	2.6369	0	0	2.778	0	2.486
D8/VANTEC	04/2004	0.2879	0	1.124	2.477	2.103	2.052
PAD V	06/2007	1.0270	0	6.640	1.237	2.693	2.109
D/MAX-B	06/2002	0.567	0	18.680	2.301	1.960	6.048
Miniflex	09/2001	5.568	0	20.47	3.614	0	5.487
PW17xx	08/1998	0	0	5.217	0	9.77	7.603

Table III. GSAS Function #3 Instrument Profile Parameters for a Variety of Laboratory Diffractometers.

Diffractometer	*U*	*V*	*W*	*X*	*Y*	*S/L*	*H/L*
X'Pert Pro PIXcel/0.04 rad Soller	1.423	0	0.5061	2.842	1.509	0.03547	0.00522
D2/Lynxeye	1.376	0	2.640	2.410	0.850	0.02951	0.0005
X'Pert Pro PIXcel/mono	1.153	-0.928	4.161	2.472	1.814	0.01577	0.0005
X'Pert Pro PIXcel/no mon	2.314	0	0	3.040	0	0.02788	0.0005
D8/VÅNTEC	0.3365	0	1.032	2.526	2.051	0.02695	0.0005
PAD V	1.103	0	6.412	1.173	2.842	0.03018	0.0005
D/MAX-B	3.219	-7.822	24.370	2.460	1.609	0.03858	0.0005

In all of these profile functions, $P = 0$.

Table IV. GSAS Profile #2 Functions for Several Synchrotron Diffractometers

Instr.	Date	*U*	*V*	*W*	*X*	*Y*	*asym*
APS 5-BM-C	10/2002	0.1	0	0	0.2505	0.9462	0
APS 5-BM-C	08/2006	17.1	-8.8	1.3	0	0	0
APS 1-ID	02/2002	0.1	0	0	0.2505	0.9462	0.0646
APS 10-ID-B	01/2000	0.3540	0	0.2908	0.3565	0.5177	0.4744
APS 32-ID	12/2004	0.3120	0	0.0104	0.1186	0.4062	0.0419
LNLS D10B		0.8777	-0.1600	0.1063	0.7604	1.1904	0.5157
NSLS X3B1	03/2004	6.427	-1.067	0	0.6102	0.6796	0.6733

Table V. GSAS Profile #3 Instrument Parameters for Several Synchrotron Diffractometers

Inst.	Date	*U*	*V*	*W*	*P*	*X*	*Y*	*S/L*	*H/L*
APS 5-BM-C	10/2002	1.212	0	0	0	1.980	0	0.00135	0.00718
APS 1-ID	02/2002	0.1	0	0	0	0.1845	11.190	0.0005	0.00458
APS 10-ID	10/2003	1.212	0	0	0	0.198	0	0.00135	0.00718
APS 11-BMB	02/2009	1.163	-0.126	0.063	0	0.173	0	0.00110	0.00110
APS 32-ID	12/2004	1.212	0	0	0	0.198	0	0.00135	0.00718
AS PD		0.0522	0.5640	0.0621	0	0.293	0.171	0.0000	0.0000
NSLS X7B		0	-125.9	73.3	0	2.03	0	0.0001	0.1000
NSLS X16C		0	0	0	1	3	30	0.014	0.014

GSAS/FullProf Conversions

$$GU(GSAS) = 1803.4U(FullProf) \quad (9)$$
$$GV(GSAS) = 1803.4V(FullProf) \quad (10)$$
$$GW(GSAS) = 1803.4W(Fullprof) \quad (11)$$
$$GP(GSAS) = 1803.4IG(FullProf) \quad (12)$$
$$LX(GSAS) = 100Y(FullProf) \quad (13)$$
$$LY(GSAS) = 100X(Fullprof) \quad (14)$$
$$S/L(GSAS) = S\_L(Fullprof) \quad (15)$$
$$H/L(GSAS) = D\_L(Fullprof) \quad (16)$$

GSAS-II

Instrument Parameters/Operations/Save Profile

More on Size and Strain

Whole powder pattern modelling: microstructure determination from powder data
Domain size and domain-size distributions
Stress and Strain

Chapters 3.6 (Leoni), 5.1 (Leoni), and 5.2 (Popa) in *International Tables for Crystallography Volume H: Powder Diffraction* (2019).

Williamson-Hall Analysis

$$\beta(d^*) = \frac{K_\beta}{\langle D \rangle} + 2ed^*$$

Integral breadth
Volume-weighted average
Lorentzian profiles

Fourier Methods (Warren-Averbach, WPPM)

$$h(s) = \int_{-\infty}^{\infty} f(y)g(s-y)\,dy$$

$$s = d^* - d^*_{hkl} = \frac{2}{\lambda}(\sin\theta - \sin\theta_{hkl})$$

$$FT[h(s)] = FT[f(s)] \times FT[g(s)]$$

Texture (Preferred Orientation)

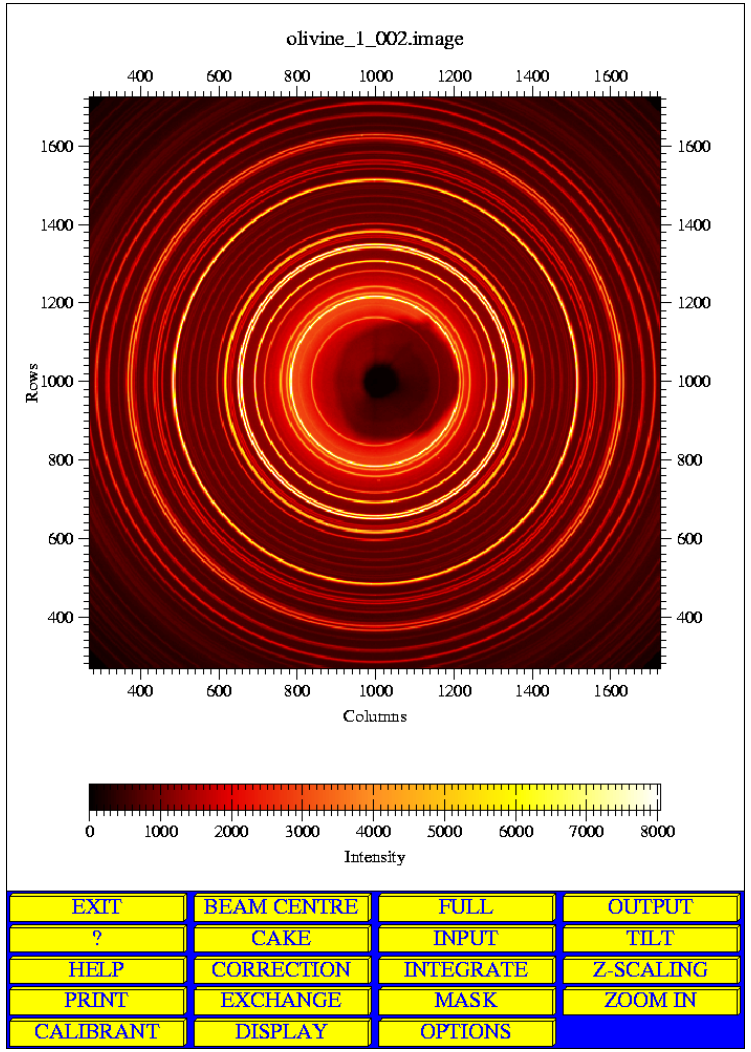

Quantitative texture analysis and combined analysis

D. Chateigner, L. Lutterotti, and M. Morales, Chapter 5.3 in *International Tables for Crystallography Volume H: Powder Diffraction* (2019).

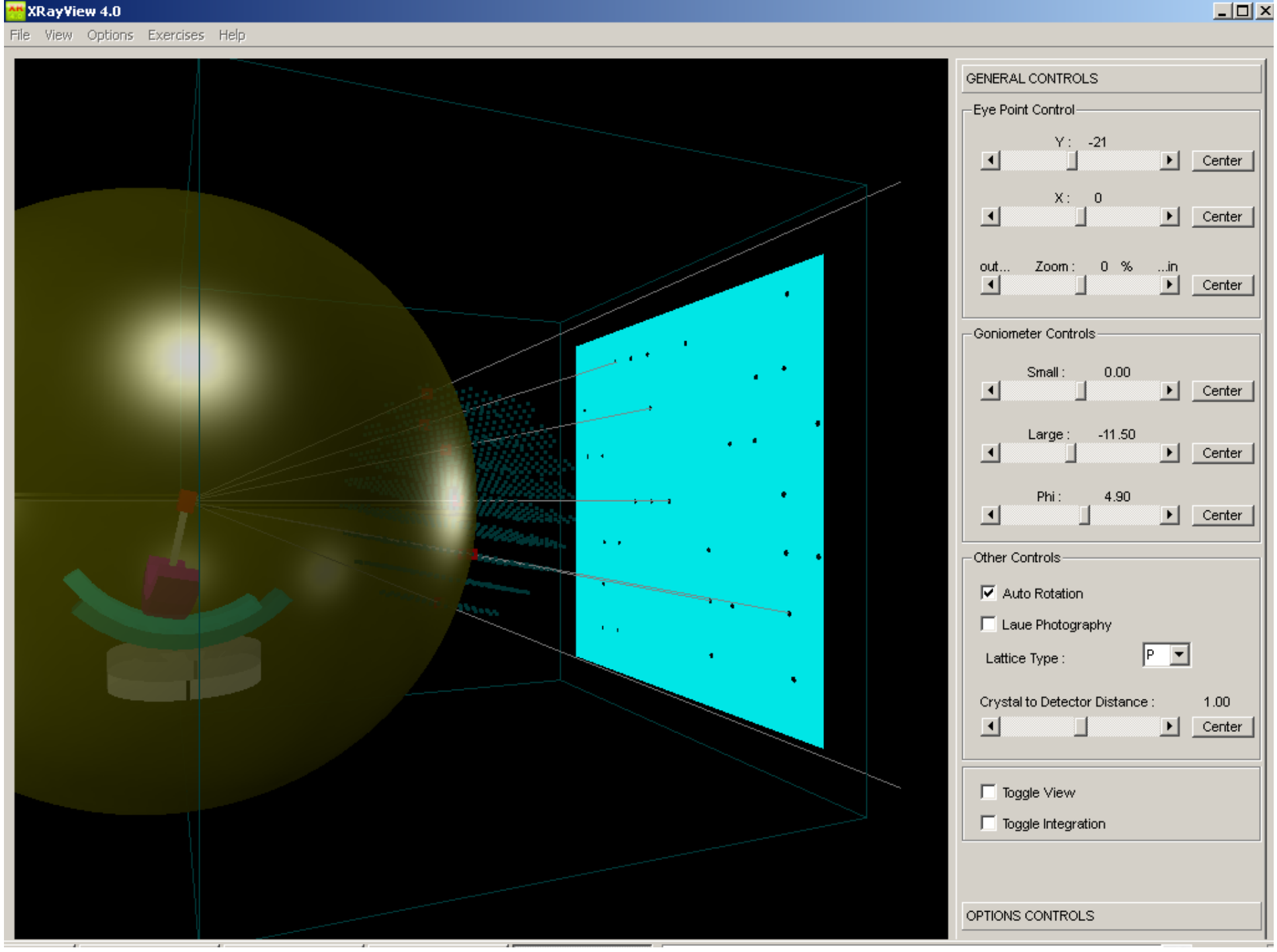
XRayView 4.0
File
View
Options
Exercises
Help
GENERAL CONTROLS
Eye Point Control
Y : -21
Center
X : 0
Center
out... Zoom : 0 % ...in
Center
Goniometer Controls
Small : 0.00
Center
Large : -11.50
Center
Phi : 4.90
Center
Other Controls
Auto Rotation
Laue Photography
Lattice Type :
P
Crystal to Detector Distance : 1.00
Center
Toggle View
Toggle Integration
OPTIONS CONTROLS

Stereographic Projection

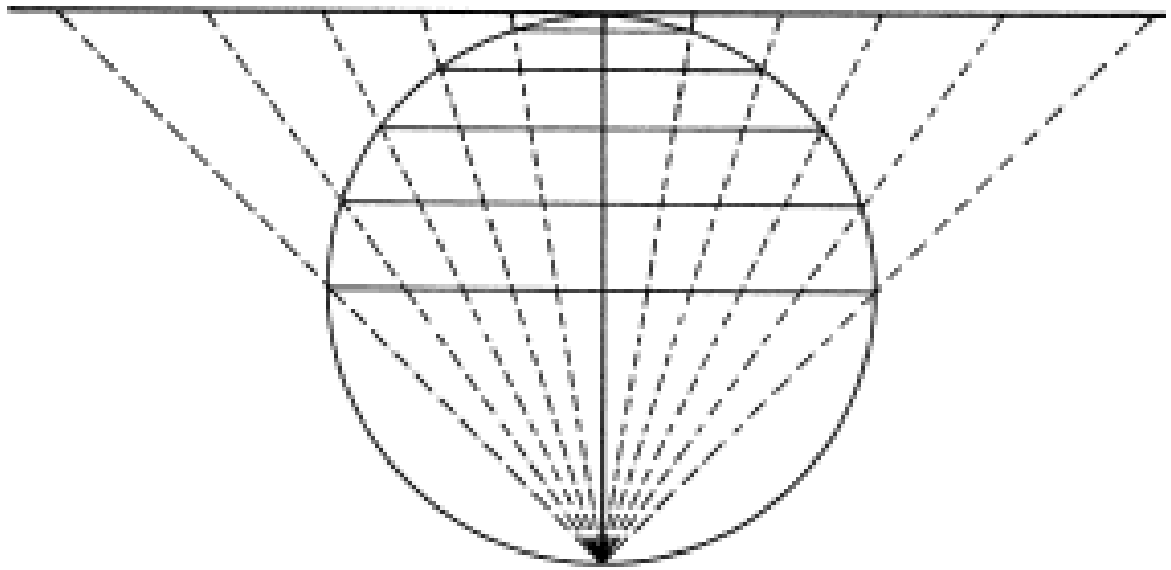

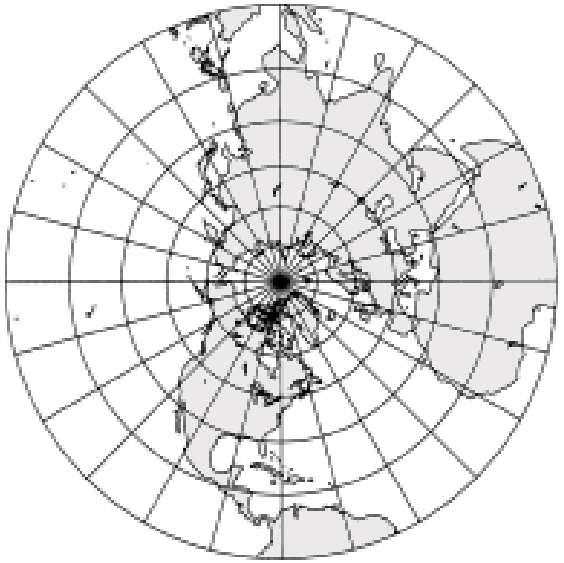

http://www.3dsoftware.com/Cartography/USGS/MapProjections/Azimuthal/Stereographic

March-Dollase Function

W. A. Dollase, “Correction of Intensities for Preferred Orientation in Powder Diffractometry: Application of the March Model”, *J. Appl. Cryst*., **19**(4), 267-272 (1986).

March-Dollase Function

$$O_{ph} = \frac{1}{M_p} \sum_{j=1}^{M_p} \left(Ratio^2 \cos^2 A_j + \frac{\sin^2 A_j}{Ratio} \right)^{3/2}$$

h_p = reciprocal lattice vector
M_p = multiplicity of h_p
A_j = angle between specified unique axis and h_p
Ratio = the refinable parameter “aspect ratio”
Cylindrical specimen symmetry assumed

BFDH Morphology - Folic Acid Dihydrate

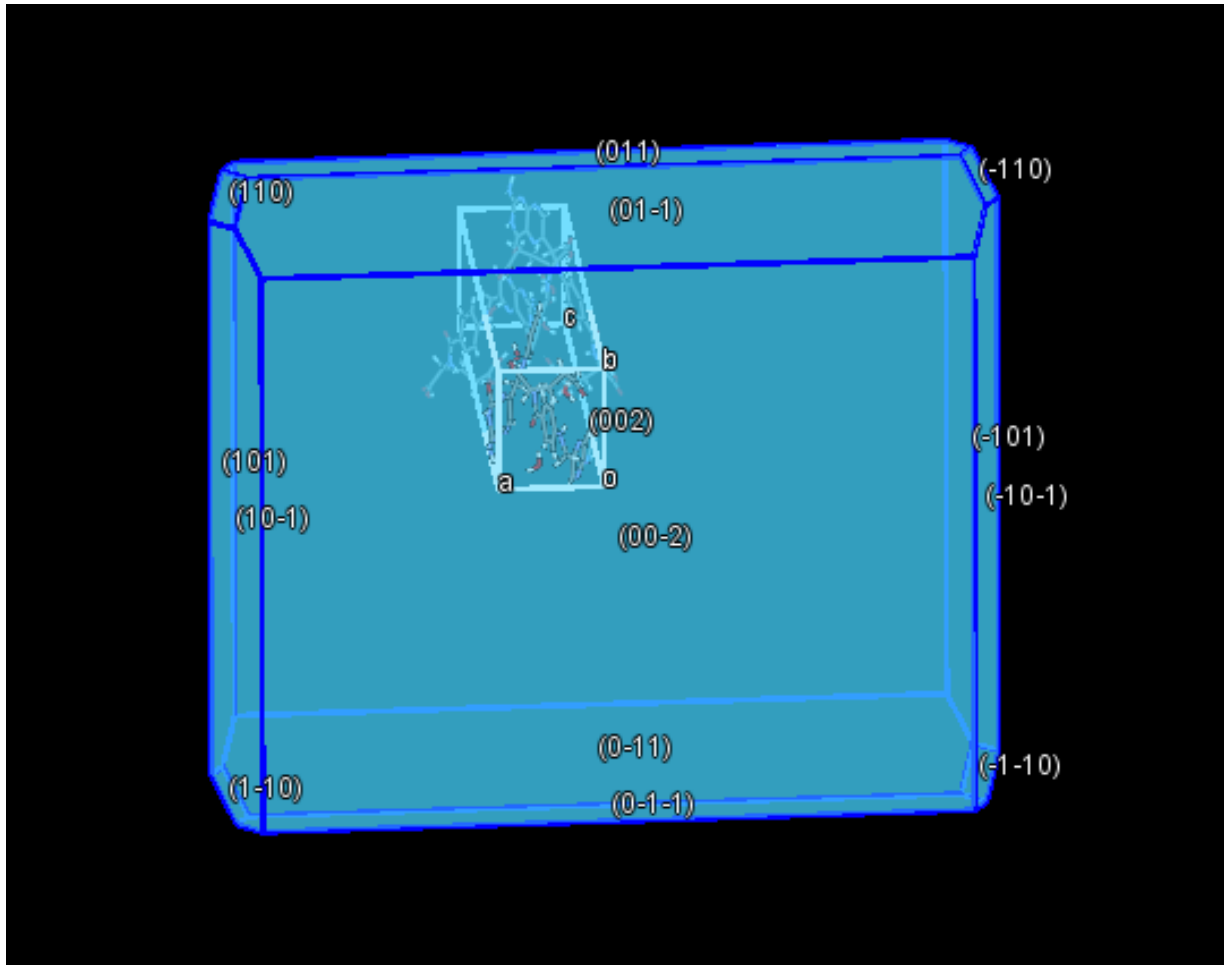

March-Dollase Function (B-B)

Plates

Ratio < 1

Oblate spheroid

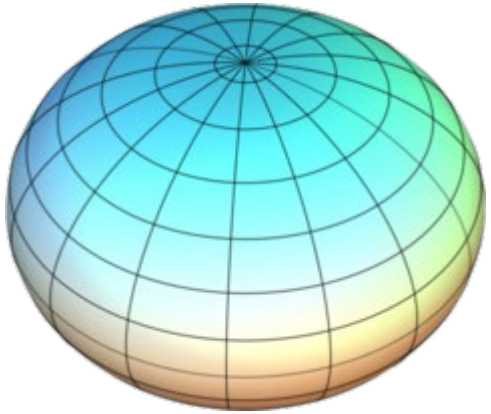

Needles

Ratio > 1

Prolate spheroid

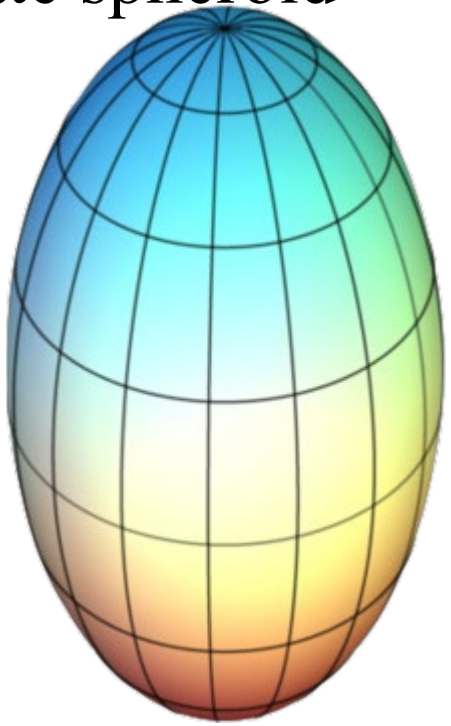

Check consistency with anisotropic broadening!

Spherical Harmonics Function

R. B. Von Dreele, “Quantitative texture analysis by Rietveld refinement”,

J. Appl. Cryst., **30**, 517-525 (1997).

Spherical Harmonics Function

$$O_p(h,y) = 1 + \sum_{L=2}^{N_L} \frac{4\pi}{2L+1} \sum_{m=-L}^{L} \sum_{n=-L}^{L} C_L^{mn} k_L^m(h) k_L^n(y)$$

Terms depend on crystal and sample symmetry

- cylindrical
- 2/m (shear)
- mmm (rolling)
- no symmetry

GSAS-II project: 3158a_1.gpx

File Data Calculate Import Export | Select tab Edit Phase | Help

- Project: C:\zjak01\ICDD_pharma
  - Notebook
  - Controls
  - Covariance
  - Constraints
  - Restraints
  - Rigid bodies
  - PWDR 11bmb_3158.fxye Ban
    - Comments
    - Limits
    - Background
    - Instrument Parameters
    - Sample Parameters
    - Peak List
    - Index Peak List
    - Unit Cells List
    - Reflection Lists
  - Phases
    - eltrombopag dioleate

General | Data | Atoms | Draw Options | Draw Atoms | RB Models | Map peaks | MC/SA | RMC | Texture | Pawley reflections

Histogram data for eltrombopag dioleate:

PWDR 11bmb_3158.fxye Bank 1

Select plot type:
- (•) None
- ( ) Mustrain
- ( ) Size
- ( ) Preferred orientation
- ( ) St. proj. Inv. pole figure
- ( ) Eq. area Inv. pole figure

[x] Use Histogram: PWDR 11bmb_3158.fxye Bank 1 ? [ ] Do new LeBail extraction?

In sequential refinement, fix these in eltrombopag dioleate for this histogram: [ ]

[x] Phase fraction: 15.7018 Wt. fraction: 1.000

Domain size model: isotropic [ ] LGmix 1.0 Reset?

[ ] size(μm): 1.0

Mustrain model: uniaxial [ ] LGmix 1.0 Reset?

Unique axis, H K L: 0 1 0

[x] Equatorial mustrain: 1262.6 [x] Axial mustrain: 1859.1

Hydrostatic/elastic strain:

[ ] D11 0.0 [ ] D22 0.0 [ ] D33 0.0

[ ] D13 0.0

[ ] Layer displacement (μm): 0.0

Preferred orientation model Spherical harmonics Harmonic order: 4 [x] Refine?

Spherical harmonic coefficients: Texture index: 1.137

C(2,-2)	-0.479	C(2,0)	0.434	C(2,2)	-0.059	C(4,-2)	-0.513
C(4,-4)	-0.137	C(4,0)	-0.294	C(4,2)	0.163	C(4,4)	-0.277

Negative MRD penalty list: [ ] Select penalty hkls Zero MRD tolerance: 0.1

[ ] Extinction: 0.0

[ ] Babinet A: 0.0 [ ] Babinet U: 0.0

Mouse RB drag/drop to reorder

Spherical Harmonics

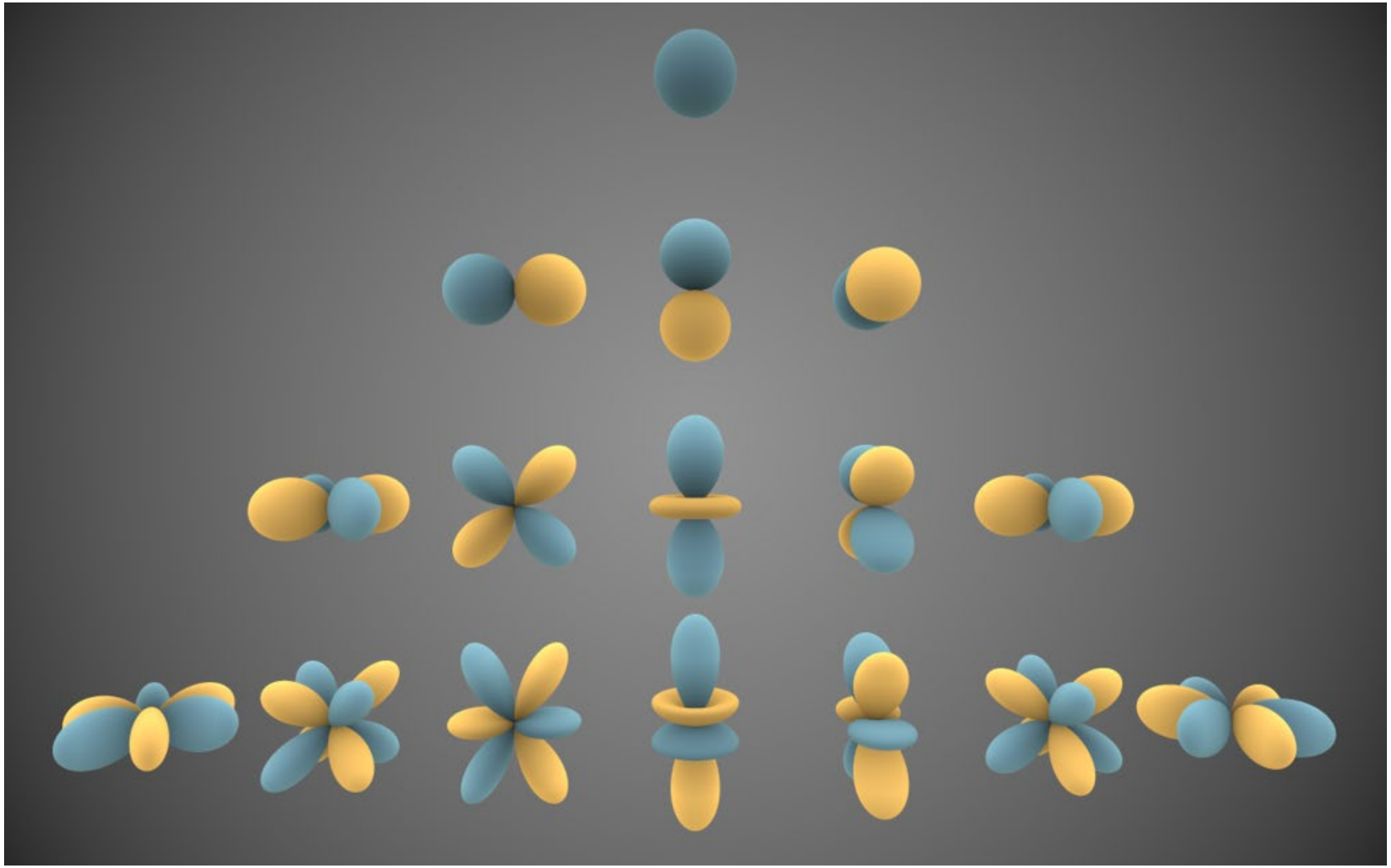

Texture Index

$$J = 1 + \sum_{L=2}^{N_L} \frac{1}{2L+1} \sum_{m=-L}^{L} \sum_{n=-L}^{L} \left| C_L^{mn} \right|^2$$

J = 1 for random

J = ∞ for single crystal

Texture Index in 11-BM Pharmaceuticals

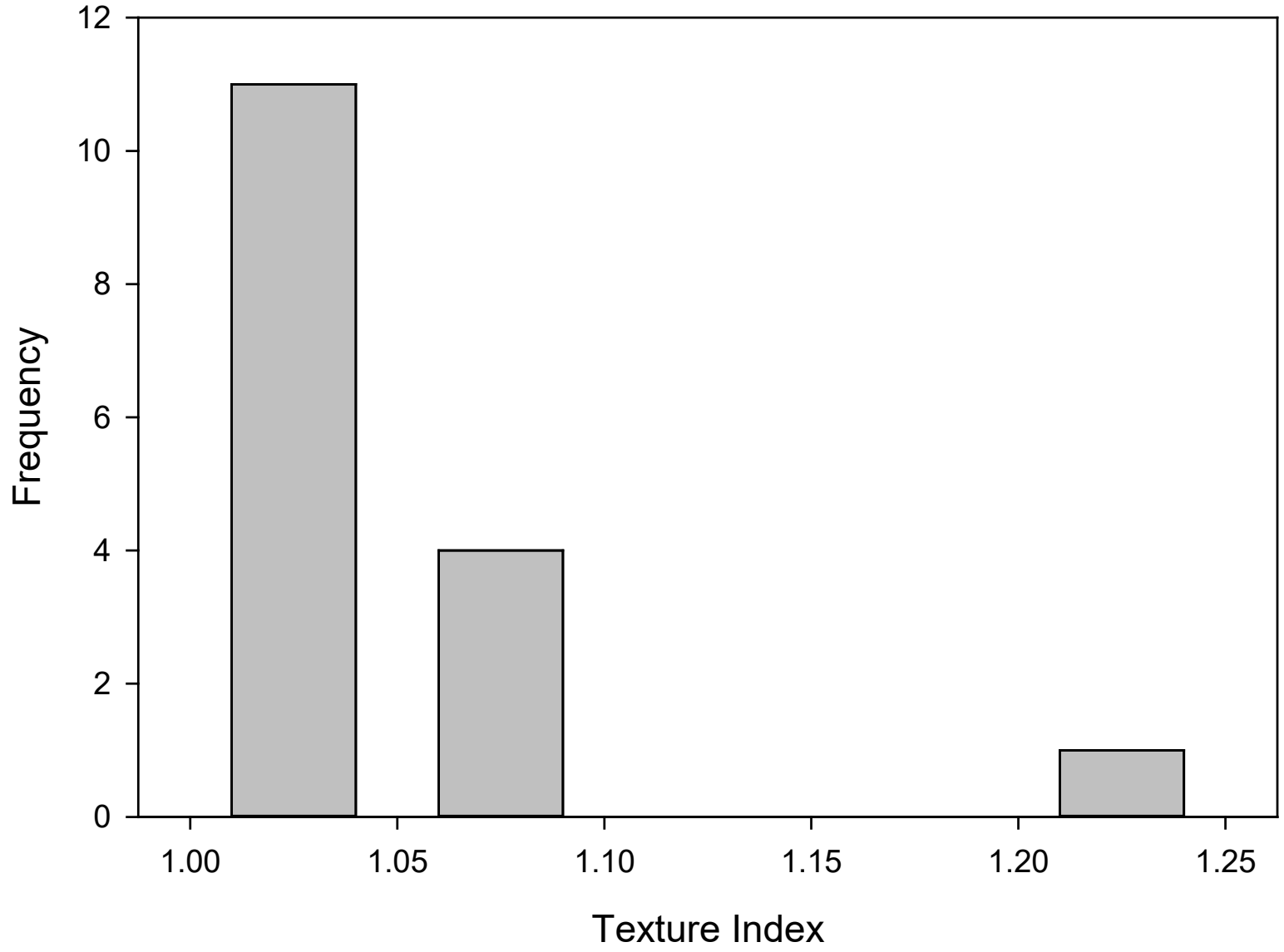

2-L PET Bottle

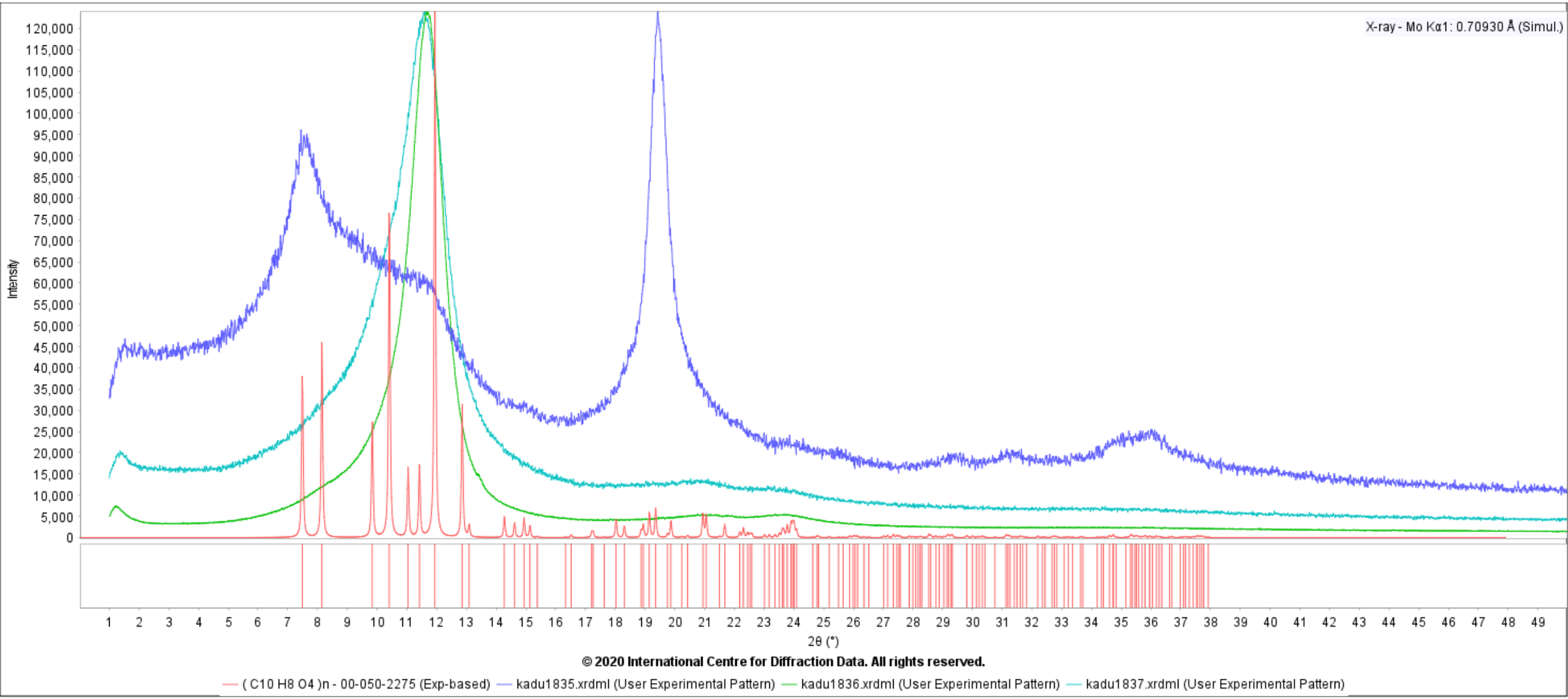
X-ray - Mo Kα1: 0.70930 Å (Simul.)
Intensity
120,000
115,000
110,000
105,000
100,000
95,000
90,000
85,000
80,000
75,000
70,000
65,000
60,000
55,000
50,000
45,000
40,000
35,000
30,000
25,000
20,000
15,000
10,000
5,000
0
1 2 3 4 5 6 7 8 9 10 11 12 13 14 15 16 17 18 19 20 21 22 23 24 25 26 27 28 29 30 31 32 33 34 35 36 37 38 39 40 41 42 43 44 45 46 47 48 49
2θ (°)
© 2020 International Centre for Diffraction Data. All rights reserved.
(C10 H8 O4)n - 00-050-2275 (Exp-based)
kadu1835.xrdml (User Experimental Pattern)
kadu1836.xrdml (User Experimental Pattern)
kadu1837.xrdml (User Experimental Pattern)

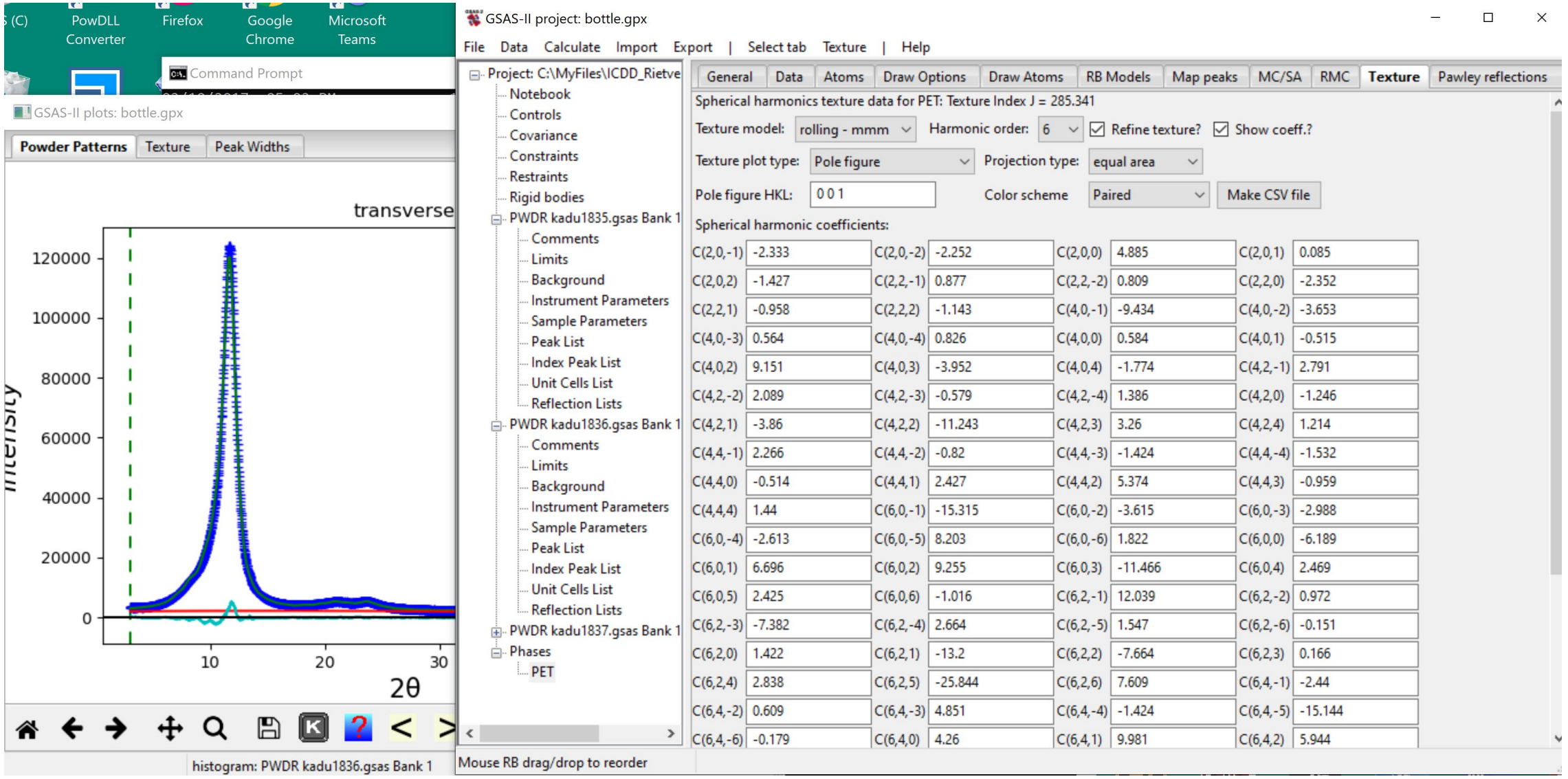
PowDLL Converter
Firefox
Google Chrome
Microsoft Teams
Command Prompt
GSAS-II plots: bottle.gpx
Powder Patterns
Texture
Peak Widths
transverse
120000
100000
80000
60000
40000
20000
0
10
20
30
2θ
histogram: PWDR kadu1836.gsas Bank 1
GSAS-II project: bottle.gpx
File
Data
Calculate
Import
Export
Select tab
Texture
Help
Project: C:\MyFiles\ICDD_Rietve
Notebook
Controls
Covariance
Constraints
Restraints
Rigid bodies
PWDR kadu1835.gsas Bank 1
Comments
Limits
Background
Instrument Parameters
Sample Parameters
Peak List
Index Peak List
Unit Cells List
Reflection Lists
PWDR kadu1836.gsas Bank 1
Comments
Limits
Background
Instrument Parameters
Sample Parameters
Peak List
Index Peak List
Unit Cells List
Reflection Lists
PWDR kadu1837.gsas Bank 1
Phases
PET
General
Data
Atoms
Draw Options
Draw Atoms
RB Models
Map peaks
MC/SA
RMC
Texture
Pawley reflections
Spherical harmonics texture data for PET: Texture Index J = 285.341
Texture model: rolling - mmm
Harmonic order: 6
Refine texture?
Show coeff.?
Texture plot type: Pole figure
Projection type: equal area
Pole figure HKL: 0 0 1
Color scheme Paired
Make CSV file
Spherical harmonic coefficients:
C(2,0,-1) -2.333 C(2,0,-2) -2.252 C(2,0,0) 4.885 C(2,0,1) 0.085
C(2,0,2) -1.427 C(2,2,-1) 0.877 C(2,2,-2) 0.809 C(2,2,0) -2.352
C(2,2,1) -0.958 C(2,2,2) -1.143 C(4,0,-1) -9.434 C(4,0,-2) -3.653
C(4,0,-3) 0.564 C(4,0,-4) 0.826 C(4,0,0) 0.584 C(4,0,1) -0.515
C(4,0,2) 9.151 C(4,0,3) -3.952 C(4,0,4) -1.774 C(4,2,-1) 2.791
C(4,2,-2) 2.089 C(4,2,-3) -0.579 C(4,2,-4) 1.386 C(4,2,0) -1.246
C(4,2,1) -3.86 C(4,2,2) -11.243 C(4,2,3) 3.26 C(4,2,4) 1.214
C(4,4,-1) 2.266 C(4,4,-2) -0.82 C(4,4,-3) -1.424 C(4,4,-4) -1.532
C(4,4,0) -0.514 C(4,4,1) 2.427 C(4,4,2) 5.374 C(4,4,3) -0.959
C(4,4,4) 1.44 C(6,0,-1) -15.315 C(6,0,-2) -3.615 C(6,0,-3) -2.988
C(6,0,-4) -2.613 C(6,0,-5) 8.203 C(6,0,-6) 1.822 C(6,0,0) -6.189
C(6,0,1) 6.696 C(6,0,2) 9.255 C(6,0,3) -11.466 C(6,0,4) 2.469
C(6,0,5) 2.425 C(6,0,6) -1.016 C(6,2,-1) 12.039 C(6,2,-2) 0.972
C(6,2,-3) -7.382 C(6,2,-4) 2.664 C(6,2,-5) 1.547 C(6,2,-6) -0.151
C(6,2,0) 1.422 C(6,2,1) -13.2 C(6,2,2) -7.664 C(6,2,3) 0.166
C(6,2,4) 2.838 C(6,2,5) -25.844 C(6,2,6) 7.609 C(6,4,-1) -2.44
C(6,4,-2) 0.609 C(6,4,-3) 4.851 C(6,4,-4) -1.424 C(6,4,-5) -15.144
C(6,4,-6) -0.179 C(6,4,0) 4.26 C(6,4,1) 9.981 C(6,4,2) 5.944
Mouse RB drag/drop to reorder

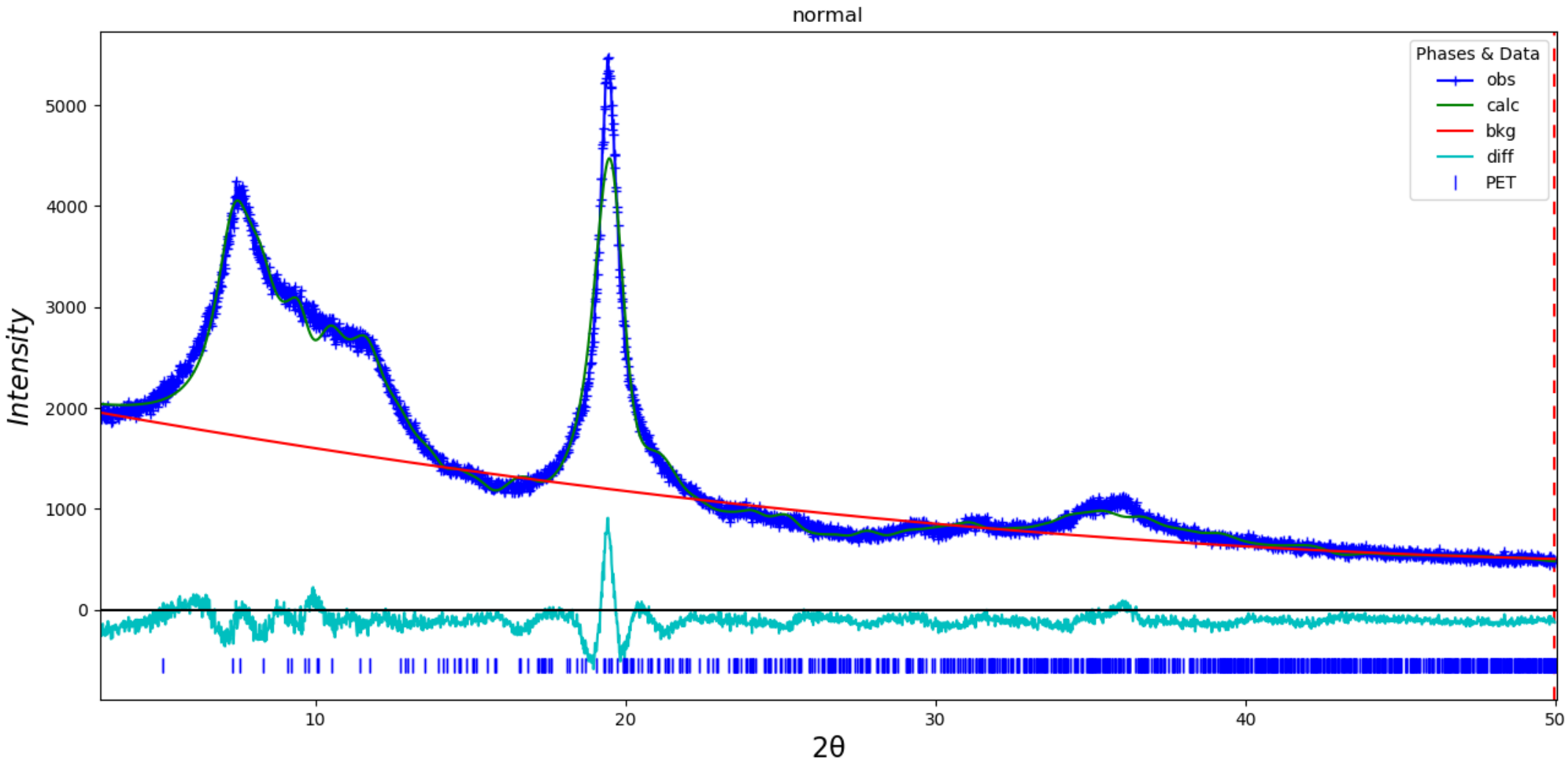
normal
Phases & Data
obs
calc
bkg
diff
PET
Intensity
5000
4000
3000
2000
1000
0
10
20
30
40
50
2θ

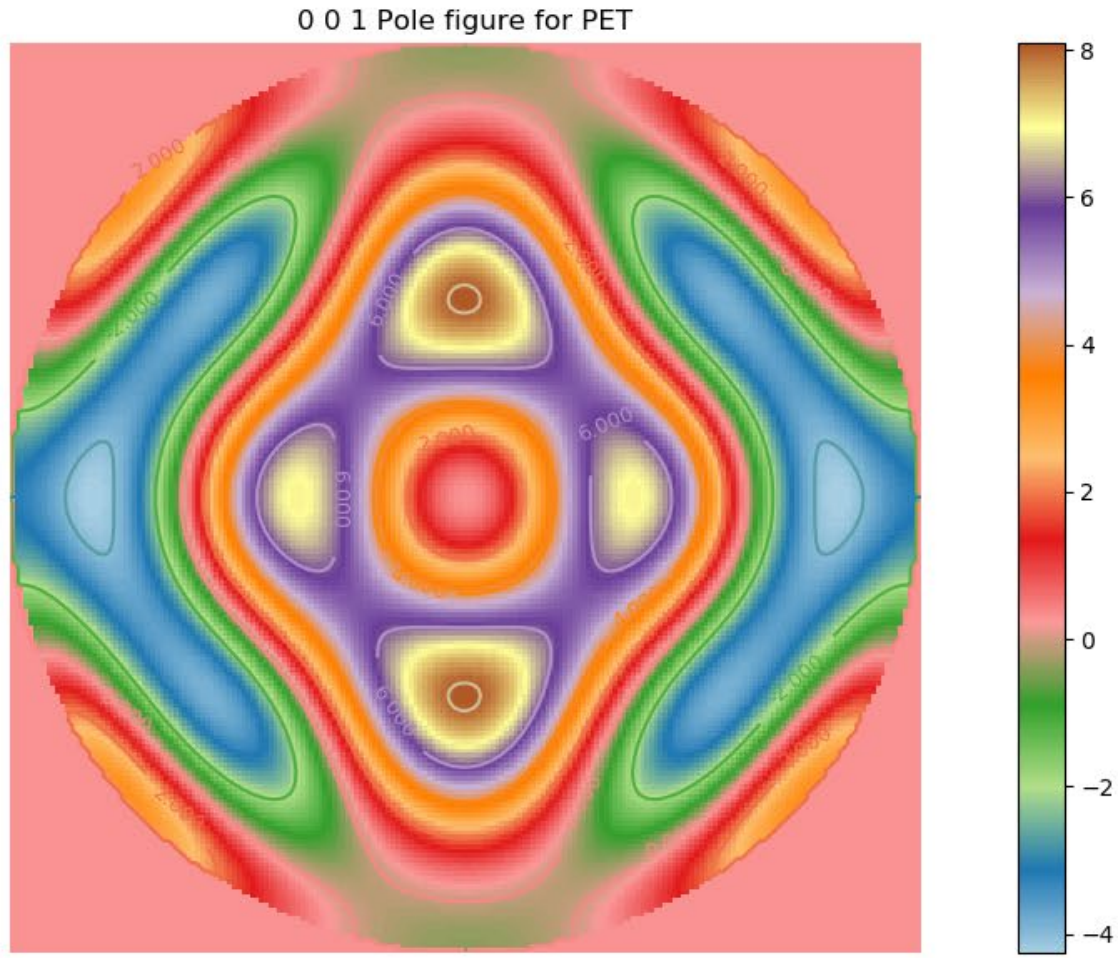
0 0 1 Pole figure for PET
8
6
4
2
0
−2
−4

Texture in HDPE Pipe